Risk-constrained bidding and offering strategy for sector-coupled electricity-hydrogen systems incorporating accessibility level of mobility sector

Zare Oskouei, Morteza; Mehrjerdi, Hasan; Palensky, Peter

Risk-constrained bidding and offering strategy for sector-coupled electricity-hydrogen systems incorporating accessibility level of mobility sector

Morteza Zare Oskouei[a,*], Hasan Mehrjerdi[b], Peter Palensky[c]

[a]*Faculty of Electrical Engineering, Sahand University of Technology, Tabriz, Iran*
[b]*Electrical & Computer Engineering Department, George Washington University, Washington, DC, USA*
[c]*Intelligent Electrical Power Grids, Delft University of Technology, 2600 Delft, The Netherlands*

Abstract

To enhance the economic viability of integrated energy systems, it is important to balance risk and reward while ensuring operational flexibility and compliance with regulatory constraints. Developing an integrated risk measurement method for energy trading in energy markets that complies with regulatory constraints adds another layer of complexity, especially when dealing with large-scale heterogeneous energy systems, such as those dominated by green hydrogen. Ensuring adherence to market regulations, grid codes, and flexible requirements requires a thorough understanding of legal frameworks and policy considerations, as well as integrating regulatory constraints into the bidding/offering strategies. To address these challenges and enable the profitable development of integrated electricity-hydrogen energy systems (IEHSs), this paper develops a risk-constrained bidding/offering self-scheduling strategy for IEHSs that allows for simultaneous trading in day-ahead energy and reserve electricity markets. The developed self-scheduling strategy regulates hydrogen and power flow in a centralized manner, taking into account the operational limits of the power sector, hydrogen fueling stations (HFSs), electric vehicle parking lots, fuel cell vehicle parking lots, and renewable energy sources. As a salient feature, the important human-related factors in the mobility sector are included in the proposed strategy to motivate private owners to collaborate with IEHSs and to accommodate the charging demand of vehicles with electricity market signals. To obtain the robust day-ahead schedule, economic risks associated with renewable power generation, calls for reserve deployment, and electricity market prices are taken into consideration. Towards this end, a stochastic adaptive robust optimization approach is proposed to control the risk of profit variability, which is solved by a nested column-and-constraint generation algorithm. The effectiveness and feasibility of the proposed strategy are verified using the modified IEEE 14-bus test system, as a standard scale of local IEHSs. The numerical results highlight the synergies impact between HFSs and the power sector, resulting in an increase in the profit of the IEHS from \$101.654k to \$275.078k. Furthermore, the IEHS can improve its profit margin and competitiveness by employing the tri-level stochastic adaptive robust optimization approach. This approach ensures that the IEHS is resistant to sudden changes in real-time interactions, even with an 8.14% increase in the imbalance cost.

Keywords: Dual optimization procedure, mobility sector, sector-coupled energy systems, stochastic

---

*Corresponding author
Email address:* `m.zare@sut.ac.ir` (Morteza Zare Oskouei)

adaptive robust approach.

₁ **Nomenclature**

A. Abbreviations

C&CG	Column-and-constraint generation.
EVs	Electric vehicles.
EVPLs	Electric vehicle parking lots.
FCs	Fuel cells.
FCVs	Fuel cell vehicles.
FVPLs	Fuel cell vehicle parking lots.
HFSs	Hydrogen fueling stations.
IEHSs	Integrated electricity-hydrogen energy systems.
KKT	Karush-Kuhn-Tucker.
MILP	Mixed-integer linear program.
RESs	Renewable energy sources.
WFs	Wind farms.

B. Sets and indices

$\mathcal{E}$	Set of EVs types, indexed by e.
$\mathcal{F}$	Set of FCVs types, indexed by f.
$\mathcal{I}$	Set of electric buses, indexed by i, j.
$\mathcal{K}$	Set of power lines.
$\mathcal{L}$	Set of EVPLs, indexed by l.
$\mathcal{M}$	Set of HFSs, indexed by m.
$\mathcal{T}$	Set of time slots, indexed by t.
$\mathcal{S}$	Set of scenarios, indexed by s.
χ	Set of the iterations of C&CG, indexed by χ'.
$\Theta_i^{\mathcal{M}}$	Set of HFSs connected to bus i.
$\Theta_i^{\mathcal{L}}$	Set of EVPLs connected to bus i.

C. Parameters and constants

$Cap_{(\cdot)}$	Capacity of EV/FCV battery.
g_{ij}, b_{ij}	Conductance/susceptance of line ij.
K_t^{r+}, K_t^{r-}	Up/down-reserve capacity coefficient requested by ISO to provide.
$P_{t,i}^{ed}, Q_{t,i}^{ed}$	Estimated hourly active/reactive demands.
SL_{ij}	Nominal capacity of power line ij.
$\widetilde{P_{t,i}^w}$	Forecasted wind power generation.
β^{pf}	Load power factor.
λ_t^{da}	Electricity price of day-ahead energy market.
$\lambda_t^{r+}, \lambda_t^{r-}$	Capacity price in the up/down-reserve markets.
ρ_t^{r+}, ρ_t^{r-}	Energy price in the up/down-reserve markets.
π_t^{re}, π^{rh}	Retail prices of electricity and hydrogen.
$\rho^{fx,hs}, \rho^{va,hs}$	Fixed and variable operating costs coefficient of hydrogen storage.
$\gamma_{(\cdot)}^{ch}, \gamma_{(\cdot)}^{dis}$	Charging/discharging rate of EVs/FCVs.

2

$\omega_{t,(\cdot)}$	Total number of EVs/FCVs that enter EVPLs/FVPLs at t.
η	Charging/discharging efficiency.
Ω_s	Probability of occurrence of each scenario.
$\mathscr{B}$	Penalty coefficient for slack variables.
$\overline{(\cdot)}, \underline{(\cdot)}$	Maxima and minima of variable $(\cdot)$.
$da, +, -$	Symbols representing participation in the energy and up/down-reserve markets.

D. Decision variables

$FL_{t,ij}, \widetilde{FL}_{t,ij}$	Active/reactive power flow of line ij.
$H_{t,m}^{ch,dis}$	Hydrogen injecting into/exporting from storage at t.
$H_{t,m}^{elv}$	Hydrogen supplied to FVPLs by electrolyzer at t.
$H_{t,m}^{fc}$	Hydrogen supplied to fuel cell at t.
$H_{t,m}^{fvpl}$	Hydrogen delivered to FVPL m at t to charge FCVs.
$H_{t,m}^{gen}$	Hydrogen produced by electrolyzer at t.
$H_{t,m}^{sv}$	Hydrogen supplied to FVPLs by hydrogen storage at t.
$P_{t,m}^{com}$	Power consumed by the compressor at t.
P_t^{da}, Q_t^{da}	Active/reactive power traded between the IEHS and the upstream grid in the energy market.
P_t^{r+}, P_t^{r-}	Power capacity traded in the up/down reserve markets.
$P_{t,m}^{el}$	Total power consumption by electrolyzer at t.
$P_{t,l}^{evpl}$	Power traded between EVPL l and IEHS.
$P_{t,m}^{fc}$	Power produced by fuel cell at t.
$P_{t,m}^{ie}$	Power consumed by electrolyzer for hydrogen generation.
$P_{t,i}^{w}$	Active power schedule of WFs.
$SOC_{t,(\cdot)}$	State-of-charge of EVs/FCVs at t.
$SOE_{t,(\cdot)}$	State-of-energy of EVPLs/FVPLs at t.
$V_{t,i}, \theta_{t,i}$	Magnitude/angle of voltage at bus i.
ν_t^{r+}, ν_t^{r-}	Binary variables denoting up/down-reserve capacity requests.
y_t^+, y_t^-	Slack variables used in the sub-problem of the C&CG algorithm.

1. Introduction

1.1. Context and motivation

Local sector-coupled energy systems enable more efficient use of resources and infrastructure Kachirayil et al. [2022]. Thanks to recent advancements in this field, the sector-coupling framework can accelerate the simultaneous trading of investors in different energy markets and also contribute to the long-term sustainability of the energy sector Zare Oskouei et al. [2021]. Due to the dynamic nature of the renewable-dominated energy systems and the dynamics of the green hydrogen trade markets, EU countries seek constructive strategies to reduce their dependence on imported fossil fuels from Russia and sustain their industrial and mobility sectors FCW [2022]. The synergies of sector coupling between electricity and hydrogen applications are considered to be the crucial strategy for the ongoing discourse over the energy crisis, contributing to the flexibility and security of supply, and inheriting the economic opportunities Yin et al. [2023]. These motivate the energy system operators to strive to turn green hydrogen, i.e.

hydrogen produced by renewable energy sources (RESs), into the major driver in the end-user supply chain, especially the mobility sector. A recent report published by the International Energy Agency (IEA) confirms that the EU has reached the initial technological maturity of the hydrogen supply chain, according to its ambitious goals. Therefore, it is expected that from 2030, green hydrogen will play an effective role in meeting the demand of the mobility sector IEA [2022]. As this trend intensifies, the power sector and hydrogen-based mobility are expected to interweave more and more, leading to the expansion of integrated electricity-hydrogen energy systems (IEHSs) Zare Oskouei & Mehrjerdi [2022]. In addition to academic research, there have been remarkable efforts in real-life to establish IEHSs, e.g., several IEHSs can be found in the UK, launched by the ITM power company ITM POWER PLC [2022].

To pave the way for the proliferation of IEHSs, the establishment of such systems, as one of the emerging players in the energy markets, must be economically justified. Towards this end, bidding/offering strategies play a central role in their sustainable development, where IEHS operators seek to maximize their profits by purposefully aggregating the capacity of different electrical and hydrogen prosumers. In this regard, two key questions ought to be addressed: 1) how can IEHS operators develop a robust market-oriented approach as an operational roadmap to take advantage of synergies of electricity and hydrogen facilities in day-ahead electricity markets? 2) how can these operators use the existing opportunities in the mobility sector in advancing their goals considering the accessibility levels of different types of vehicles?

1.2. Relevant background

A market-oriented approach for energy systems should be developed in such a way that the bid curve, i.e., providing energy to markets, and/or offer curve, i.e., buying energy from markets at low prices, optimally meet the objectives of the system operator. The existing literature on the strategic bidding and offering of IEHSs can be categorized into two groups based on whether or not the operational limits of the power sector are considered in line with the market-oriented approaches. A wide variety of literature in the field has been devoted to the latter, e.g., see Firtina-Ertis et al. [2020]; Li et al. [2020]; Xiao et al. [2018]. In those studies, authors concentrated on developing profit-driven strategies to assess the value of IEHSs in day-ahead energy and reserve markets considering RESs, electric vehicles (EVs), fuel cell vehicles (FCVs), and fuel cells (FCs). According to the strong evidence presented by the Federal Energy Regulatory Commission (FERC), the importance of modeling the soft and hard operational constraints of power grids in deriving electricity market participation models for energy system owners, e.g., IEHS operators, is essential Sauer [2014]. Recall that besides making profits in day-ahead electricity markets, an IEHS operator is also concerned with meeting end-users at satisfactory operating standards. Ignoring operational constraints of IEHSs' components, especially the power sector, market-based approaches can leave them open to technically infeasible results in practice. Furthermore, these studies did not consider the dynamics power and hydrogen system, as well as the mobility sector activity schedules, when developing the bidding/offering strategy for IEHSs. This makes it impossible to practically implement IEHSs in the broader energy landscape and to reach optimal solutions in real-time sessions.

In contrast, there are studies that made a step further by discussing how the power sector operational limits affect the IEHSs bidding/offering problems by fulfilling the grid code requirements. For instance, authors in El-Taweel et al. [2019] proposed a deterministic self-scheduling method to increase the profit

of IEHSs by serving the FCVs and participating in the day-ahead electricity market while meeting the technical constraints of the power sector. In the same study, the hydrogen fueling stations (HFSs), including electrolyzer, FC, and hydrogen storage, were used to minimize the renewable power curtailment and exploit the lower market prices. In Tao et al. [2021], a deterministic price-based unit commitment approach was presented to devise the profitable offering strategy of IEHSs in a day-ahead electricity market; where the supply chain for hydrogen was considered incomplete. In Ban et al. [2017], an energy trading scheme was developed for the IEHSs to participate in the day-ahead energy market to justify the economic viability of the HFSs, as the main coupling points of the electricity and hydrogen sectors. The work reported in Shao et al. [2021] presented a risk-averse optimal operation of IEHSs to derive the bidding strategy in the day-ahead energy market to serve the required energy on-site for FCVs, wherein uncertainties of market price and renewable power production were modeled by the selection of appropriate scenarios. Likewise, a stochastic network-constrained strategy was presented in Haggi et al. [2021] to address the bidding strategy of IEHSs in the day-ahead electricity market to exploit arbitrage opportunities arising as a result of the electricity market price volatility using FC and hydrogen storage systems. Nevertheless, the critical service design parameters of the mobility sector were seldom considered in that study. To enhance the holistic operation efficiency of IEHSs and promote a more balanced distribution of power flow, studies such as Sun et al. [2022] investigated the IEHSs bidding and offering strategies in the day-ahead energy market using a coordinated operation strategy. Authors in Li et al. [2022] argued that the deployment of HFSs is required to derive a least-cost bidding strategy for IEHSs, aiming to supply the hydrogen demands of the mobility sector alongside the electrical demands at the regional scale. The simulation results demonstrated that increasing the number of coupling points, i.e., HFSs, in interconnected local energy systems is a critical step during the transition towards a 100% renewable energy system. Authors in Khani et al. [2020] developed a supervisory-based model to optimally schedule HFSs within the framework of the renewable-dominated power grids to coordinate the trading of electricity in both energy and reserve electricity markets. In that study, the authors tried to provide operating reserve capacity to electricity markets and supply FCVs considering the constraints of the power grids and market signals, thereby maximizing the economic viability of the IEHSs. In Zhang et al. [2022] a market-oriented framework was proposed for hydrogen providers to opportunistically trade electricity and hydrogen in energy and reserve markets.

Integrated risk measurement methods and windfall profit-aware approaches for energy trading play an important role in the establishment of IEHSs from an economic planning perspective. Several studies, including those referenced in Li et al. [2023] and Mu et al. [2022], have presented risk management strategies for making profitable decisions in integrated energy systems by relying on high-power RESs. In Xiao et al. [2024], a windfall profit-aware stochastic scheduling model was presented considering the integrated risk-seeking and risk-averse preference of industrial virtual energy systems for participating in day-ahead and real-time electricity markets. Furthermore, in Xuan et al. [2021], a risk measurement method was proposed to manage potential high profits and extreme losses in integrated energy systems using conditional value at risk (CVaR); wherein, the static energy storage systems and high-power RESs were employed to minimize potential risks.

A detailed comparison of the aforementioned literature is summarized in Table 1. According to the technical literature, there remain three major limitations in the IEHSs' bidding/offering strategies that necessitate further studies. **At first**, although some studies, e.g., Khani et al. [2020]; Zhang et al. [2022], have explored bidding/offering strategies for energy and reserve markets within the context of IEHSs, there is a dearth of studies that systematically analyze and exploit the impact of energy and reserve trading floor dynamics on utilizing the potential capacity of various components of IEHSs to enhance the market penetration of IEHSs. In addition, the existing bidding/offering models for IEHSs often overlook the power and hydrogen system dynamics and the operational constraints specific to the under-operation area of IEHSs when submitting bids and offers to energy and reserve markets, hindering their effectiveness and scalability. From the perspective of the market mechanism, bids and offers from private energy systems, specifically IEHSs, must be simultaneously submitted in the day-ahead energy and reserve markets in most markets, e.g., the Ontario electricity market. These bids and offers must consider the soft and hard operational constraints related to the network operated by each entity. **Second**, there is no single study that has simultaneously considered the uncertainties of calls for reserve service, renewable power, and electricity market prices for evaluating economic risks in IEHSs, taking into account non-parametric optimization approaches, e.g., robust or information-gap decision theory approaches. Some scholars, e.g., Haggi et al. [2021]; Shao et al. [2021], only focus on the uncertainties of electricity market price and renewable power generation considering pure stochastic-based techniques. Since stochastic programming requires historical data of the probability distribution functions, which may not be always available, therefore, by modeling all uncertainties through stochastic programming, operators may miss proper scheduling for malicious scenarios that can have serious adverse effects on the IEHSs Akhavan-Hejazi & Mohsenian-Rad [2018]. **Last but not least,** existing studies did not incorporate the operating parameters of the mobility sector as well as the economic interests and activity schedules of vehicle owners in the modeling of market-oriented plans of IEHSs. Existing studies often overlook the nuanced behaviors and preferences of vehicle owners, leading to oversimplified assumptions that may not accurately reflect real-world dynamics. One of the main criticisms of existing strategies is the unrealistic assumption that different types of FCVs, e.g., buses and taxis, are charged at the same hydrogen pressure level. Another unrealistic assumption is that the accessibility level of IEHS operators to different types of vehicles was assumed to be the same. The latter assumption oversimplifies the behavior of private owners and explicitly sacrifices owners to maximize the profits of IEHS operators in energy markets. In practice, EVs and FCVs belong to different owners with different behavioral characteristics. These owners are more concerned with their own interests, instead of interacting with IEHSs. Therefore, it is necessary to achieve a holistic approach that enhances the realism and effectiveness of market-oriented plans for IEHSs in the presence of the mobility sector. This will ultimately facilitate more sustainable and efficient energy management practices.

In summary, our work is somewhat related to Khani et al. [2020]; Zhang et al. [2022], which developed bidding/offering strategies for the participation of IEHSs in energy and reserve markets. Nevertheless, these studies did not consider the impact of the mobility sector on the developed bidding/offering strategies. Also, the uncertainties of calls for reserve service and electricity market prices were not involved by

Table 1: Taxonomy of literature in the field.

Ref.	Trading markets		IEHS uncertainties			Risk modeling method	Accessibility level of mobility sector
	Energy	Reserve	RESs power	Market prices	Calls for reserve		
El-Taweel et al. [2019]	✓	×	×	×	×	×	×
Tao et al. [2021]	✓	×	×	×	×	×	×
Shao et al. [2021]	✓	×	✓	×	×	SA	×
Haggi et al. [2021]	✓	×	✓	✓	×	SA	×
Sun et al. [2022]	✓	×	✓	×	×	×	×
Li et al. [2022]	✓	×	×	×	×	×	×
Khani et al. [2020]	✓	✓	×	×	×	×	×
Zhang et al. [2022]	✓	✓	✓	×	×	SA	×
This study	✓	✓	✓	✓	✓	SARA	✓

Note: SA-Stochastic approach; SARA-Stochastic adaptive robust approach

Khani et al. [2020]; Zhang et al. [2022] to obtain a risk-averse trading framework.

1.3. Technical contributions and paper structure

In light of the aforementioned research gaps, the formative contributions of this study can be expressed as follows:

1. *Facilitating the commercialization of IEHSs by developing a trackable and robust market-oriented framework to integrate different trading floors of energy markets while satisfying local grid code requirements*—this paper aims to develop the coordinated bidding/offering problem for IEHSs, involving HFSs, RESs, electric vehicle parking lots (EVPLs), and fuel cell vehicle parking lots (FVPLs) to trade in day-ahead energy and up/down reserve electricity markets. To the best of the authors' knowledge, it is fair to say that this is the first attempt that tries to investigate the influence of the level of access to the mobility sector as well as the energy and reserve trading floor dynamics and their impact on the market penetration of IEHSs, highlighting strategies to leverage these dynamics to enhance IEHSs' participation and profitability in energy markets. In this regard, we address the critical issue of privacy preservation by developing novel protocols and mechanisms to safeguard IEHSs' operational data while enabling collaboration with energy market operators for market participation. We present a scalable robust optimization algorithm to address the strategic bidding/offering problem, where our methodology is customized to exploit the capacities of mobility sector in such problems, in contrast to Khani et al. [2020]; Zhang et al. [2022]. More specifically, the developed approach addresses most of the challenges in solving large self-scheduling problems for finding the strategic bidding/offering equilibrium in such a way that a reliable and computationally tractable approach is derived for IEHS operators from a modeling and programming perspective. The power and hydrogen generation, storage, and delivery processes are optimized considering HFSs operational constraints coordinated with variable RESs and constrained power sector operations.

2. *Establishing a coherent decision-making framework to mitigate the risk posed by soft and hard uncertainties on the economic interactions of IEHSs in energy markets*—because the decisions to be made by IEHS operators involve a significant level of data uncertainty, realistic operational condi-

tions must be included in the bidding/offering process to ensure that market participation does not jeopardize the quality of service in IEHSs. To this end, the strategic bidding/offering problem is mathematically formulated as a tri-level stochastic adaptive robust optimization problem to obtain risk-averse and robust solutions in facing ubiquitous soft and hard uncertainties. Hereupon, the presented method in this study is fundamentally different from the studies in the literature, e.g., due to the need to achieve a unique tri-level optimization model to handle uncertainty signals governing the energy and regulation-up and down reserve markets, which play an undeniable role as economic levers in the risk-embedded scheduling of IEHSs. In the context of IEHSs, where decisions have to be made under significant data uncertainty, it is crucial to adopt a methodology that can effectively handle this uncertainty while ensuring the robustness and quality of service in the system. In the proposed risk-constrained bidding/offering strategy for IEHSs, the adaptive robust optimization method and stochastic approach are integrated to reduce optimization problem complexity. This is achieved by identifying soft and hard uncertainties and separately implementing risk management strategies. The stochastic adaptive robust optimization approach focuses on hard uncertain sources as they significantly impact the decision-making process. However, the operator does not need to pay an excessive fee to control the soft uncertain parameters, and the risk caused by these parameters can be managed by utilizing the stochastic approach. Hence, the inclusion of risk constraints in the stochastic adaptive robust optimization framework allows for the consideration of risk-averse behavior, ensuring that the bidding/offering strategies prioritize the mitigation of potential risks associated with market participation. This means that the optimization decisions are made to be robust against a set of uncertainty scenarios without requiring precise probability distributions, thereby providing flexibility in handling different levels of data uncertainty. Furthermore, by formulating the bidding/offering problem as a tri-level stochastic adaptive robust optimization approach, operators ensure that realistic operational conditions are incorporated into the optimization process. This helps prevent situations where market participation could compromise the quality of service in IEHSs. To develop a computational framework that can guarantee a feasible and global optimal solution, we go through numerous steps based on both the Karush-Kuhn-Tucker (KKT) optimality conditions and convex optimization techniques. By so doing, the developed unified energy and reserve decision-making process boil down to solving tractable mixed-integer linear program (MILP).

3. *Respecting the accessibility level of mobility sector*—the distinctive feature of the proposed strategy is to add pure realism to the existing literature, e.g., Khani et al. [2020]; Zhang et al. [2022], by considering the behavior of different types of EVs and FCVs and their utility functions in the bidding/offering strategy of IEHSs. This ensures that the realization of the interests of the IEHS operators in the energy markets will not jeopardize the vehicles owners' welfare. Without loss of generality, multiple realism cases, such as private owners' activity schedules and the accessibility level of IEHS operators to different types of vehicles in various parking lots, are reflected in the market-oriented strategy by monitoring the charging behaviors of parking lots.

The remainder of this article is organized as follows. Section 2 introduces the architecture of IEHSs and integrated energy system components. Section 3 is devoted to introducing the proposed stochastic adaptive robust optimization approach for the bidding/offering strategy of IEHSs, and the corresponding solution procedure is presented in Section 4. The simulation results conducted on case studies are discussed in Section 5. Finally, Section 6 concludes the paper and provides directions for further research.

2. Architecture of IEHSs

IEHSs are typically created by merging power sectors, which can be modeled by a tree topology graph $(\mathcal{I}, \mathcal{K})$, the set $m = \{1, ..., \mathcal{M}\}$ of $\mathcal{M}$ HFSs, wind farms (WFs), EVPLs, and FVPLs, such as the one in Fig. 1. Let $i = \{1, ..., \mathcal{I}\}$ denote the set of electric buses, bus 1 as the point of common coupling. Each pair (i, j) in $\mathcal{K}$ denotes a power line. The IEHS operator is responsible for the operation of the power network under its cover, ensuring that all individual consumers and mobility sector in the area have reliable access to electricity and hydrogen with the highest level of flexibility. For this purpose, the IEHS operator tries to provide required service access to consumers and the mobility sector by using its own local energy production equipment, i.e., WFs and HFSs, as well as by participating in the energy and regulation-up and down reserve markets, taking into account economic and technical considerations. HFSs contain sets of electrolyzer, FC, and hydrogen storage units that are energized by the power sector to 1) serve on-site energy for FVPLs by electrolyzers at the current time interval or by reserved hydrogen in storage units at previous time intervals; and 2) provide operating reserve services through supplying power back to the reserve electricity market. It should be mentioned that the IEHS operator is responsible for satisfying the technical constraints in the areas under its control.

The main objective of this study is to develop a risk-constrained market-oriented self-scheduling strategy for IEHSs that submit offers/bids in day-ahead energy and reserve electricity markets, taking into account all critical uncertain sources. The IEHS operators submit bids and offers to markets based on production and storage resource information within the IEHS, following an adaptive robust risk management strategy. For this purpose, the rules of two-settlement electricity markets, e.g., CAISO and PJM, can be adopted during the proposed market-oriented strategy. In these markets, the energy and reserve markets are cleared a day before the operating day and it takes one hour and 30 minutes to clear the energy and reserve markets, respectively. In this article, to coordinate the market clearing time scale of both markets, the scheduling time slot is considered to be 30 minutes. As it was mentioned, the formed IEHS is connected to the upstream grid via the point of common coupling (PCC), whose dimension is much smaller than that of the rest of the energy network. Hence, the most *crucial prerequisite* for implementing the proposed bidding/offering strategy is that the IEHS is considered as a *price-taker* entity in the electricity markets. That means the bidding/offering strategy of IEHS does not affect the day-ahead electricity market price. IEHS operators must submit the non-priced quantity bid (or supplier offer) curve for the next 24 hours. In summary, the developed framework aims to determine the optimal and strategic bidding/offering equilibrium for the IEHSs in the day-ahead energy and reserve markets. This is achieved through the tri-level stochastic adaptive robust optimization approach that considers the effective uncertainties. The outputs of the self-scheduling problem are then submitted to the ISO. It is important to note

Fig. 1: Schematic illustration of a typical IEHS.

that the developed structure does not address the dispatch problem related to the ISO side. The economic profit of the IEHS can be maximized by deriving the integrated bidding/offering decisions for individual entities under the supervision of the IEHS operator, e.g., HFSs, EVPLs, and FVPLs. Considering the behaviors of the mobility sector's actors, i.e., owners of EVs and FCVs, in the strategic bidding/offering problem can have a significant impact on the IEHS operators' decisions. To attract the owners of EVs and FCVs to opt-in the IEHSs' market-oriented programs, it is essential to consider their utility functions based on the specific observed behaviors of different owners in the submitted bids/offers. The sequence of stages to be considered for IEHS operator decision-making is as follows:

Sequence 1: This stage is to gather the historical data for RESs generation, energy and reserve prices, behavior patterns of parking lots, and electrical demand of individual consumers, afterward to estimate these values based on the collected data for the next day.

Sequence 2: This stage is to execute the proposed bidding/offering strategy by the IEHS operator and to send out the scheduling setpoints to the day-ahead energy and reserve electricity markets, EVPLs, FVPLs, and HFSs (refer to *Section* 3). The results of the self-scheduling process must be approved by the operator so as not to violate the operational constraints of the IEHS, e.g., nominal rating of power lines, voltage limits, and so on. Fig. 2 illustrates the decision process of IEHSs, taking into account the actual time frame of electricity market operation.

2.1. HFSs modeling

The operational constraints of HFSs can generally include many details, c.f. Shao et al. [2021]. The most dominant operational constraints of HFSs, which refer to hydrogen generation/storage/consumption level by electrolyzer/hydrogen storage/FC based on converting factors, can be expressed by (1)-(5). Given the widespread adoption of Proton Exchange Membrane (PEM) electrolyzers in various energy applications, including green hydrogen production, industrial applications, and the mobility sector, this type of electrolyzer is chosen for hydrogen production in the context of HFSs. The efficiency of a PEM elec-

10

Fig. 2: IEHSs decision-making process according to the time frame of electricity market operation.

trolyzer can be affected by various factors, including operating temperature, pressure, electrode materials, and electrolyte composition. In general, PEM electrolyzers operate at relatively low temperatures (typically $50 - 80°C$) and require a source of electrical power to drive the electrolysis process. Under the proposed strategy, the IEHS operators use WFs to run the electrolysis process and produce green hydrogen ($H_{t,m}^{gen}$). In order to formulate the proposed risk-constrained market-oriented strategy for IEHSs and ease the mathematical analysis of the tri-level optimization model, a constant efficiency is considered for PEM electrolysis. It allows for the use of constant parameters in the equations, which can make dual computations more manageable and reduce the complexity of optimization algorithms. This assumption is also based on empirical studies and manufacturer's specifications, which indicate that PEM electrolyzers have relatively stable efficiencies under normal operating conditions Shao et al. [2021]. Therefore, the hydrogen conversion efficiency of the electrolyzer, i.e., κ^{E2H}, is considered to be 16.67 kg/MWh Shao et al. [2021]. Ordinarily, the hydrogen required in the mobility sector must be provided at two different pressure levels, i.e., 450 and 900 bar, for which a high-pressure compressor (HPC) and low-pressure compressor (LPC) should be used. Based on (2), the electricity used to compress hydrogen can be calculated using parameters κ^{H2C1} and κ^{H2C2}. Constraints (4)-(8) satisfy the mass balance of hydrogen at each HFS ($SOC_{t,m}^{hs}$) according to the economic signals emanating from the bidding/offering problem. These equalities imply that in each HFS, the hydrogen demand of FCVs ($H_{t,m}^{fvpl}$) is equal to electrolyzer generation ($H_{t,m}^{elv}$) plus net hydrogen inflows from hydrogen storage minus FC consumption ($H_{t,m}^{fc}$). Constraints (9) and (10) enforce hydrogen generation and consumption limits by the electrolyzer and FC, respectively. The mass of hydrogen stored in the storage units at each time slot as well as the input and output hydrogen flow limits of the reservoir are enforced by (11)-(13).

It's worth noting that the variables after each colon in the presented equations indicate dual variables corresponding to each constraint. This is also true for the following sections.

$$\kappa^{E2H} \cdot P_{t,m}^{ie} = H_{t,m}^{gen} : \quad \gamma_{t,m}^1, \quad \forall t, m, \tag{1}$$

$$\begin{cases} \kappa^{H2C1} \cdot H_{t,m}^{gen} = P_{t,m}^{com}, & \forall t, m : \text{LPC(450bar)} \\ \kappa^{H2C2} \cdot H_{t,m}^{gen} = P_{t,m}^{com}, & \forall t, m : \text{HPC(900bar)} \end{cases} \tag{2}$$

$$P_{t,m}^{ie} + P_{t,m}^{com} = P_{t,m}^{el} : \quad \gamma_{t,m}^2, \quad \forall t, m, \tag{3}$$

$$SOC_{t,m}^{hs} = 0.95 \cdot SOC_{t-1,m}^{hs} + \frac{\eta^{ch} H_{t,m}^{ch} \Delta t}{Cap^{hs}} - \frac{H_{t,m}^{dis} \Delta t}{\eta^{dis} Cap^{hs}} : \quad \gamma_{t,m}^4, \quad \forall t, m, \tag{4}$$

11

$$\kappa^{H2E} \cdot H_{t,m}^{fc} = P_{t,m}^{fc} : \quad \gamma_{t,m}^{7}, \quad \forall t, m, \tag{5}$$

$$H_{t,m}^{ch} + H_{t,m}^{elv} = H_{t,m}^{gen} : \quad \gamma_{t,m}^{3}, \quad \forall t, m, \tag{6}$$

$$H_{t,m}^{sv} + H_{t,m}^{fc} = H_{t,m}^{dis} : \quad \gamma_{t,m}^{5}, \quad \forall t, m, \tag{7}$$

$$H_{t,m}^{sv} + H_{t,m}^{elv} = H_{t,m}^{fvpl} : \quad \gamma_{t,m}^{6}, \quad \forall t, m, \tag{8}$$

$$\underline{H^{gen}} \le H_{t,m}^{gen} \le \overline{H^{gen}} : \quad \gamma_{t,m}^{8\uparrow}, \gamma_{t,m}^{8\downarrow}, \quad \forall t, m, \tag{9}$$

$$\underline{H^{fc}} \le H_{t,m}^{fc} \le \overline{H^{fc}} : \quad \gamma_{t,m}^{9\uparrow}, \gamma_{t,m}^{9\downarrow}, \quad \forall t, m, \tag{10}$$

$$\underline{SOC^{hs}} \le SOC_{t,m}^{hs} \le \overline{SOC^{hs}} : \quad \gamma_{t,m}^{10\uparrow}, \gamma_{t,m}^{10\downarrow}, \quad \forall t, m, \tag{11}$$

$$0 \le H_{t,m}^{ch} \le \frac{\overline{H^{ch}}}{\eta^{ch}} : \quad \gamma_{t,m}^{11\uparrow}, \quad \forall t, m, \tag{12}$$

$$0 \le H_{t,m}^{dis} \le \frac{\overline{H^{dis}}}{\eta^{dis}} : \quad \gamma_{t,m}^{12\uparrow}, \quad \forall t, m. \tag{13}$$

2.2. Mobility sector modeling

The IEHS operators can access a significant amount of power storage when the EVs are parked in the EVPLs. On the other hand, the IEHS operators have the duty to meet the hourly hydrogen demand of FCVs parked in the FVPLs. It should be noted that the FVPLs only operate in charging mode. The availability and adequacy of power storage and changes in hydrogen demand are strongly dependent on some important human-related factors and the physical characteristics of the vehicles: the variety of arriving and parked vehicles at each time slot, activity schedules of vehicle owners, arrival state of charge (SoC), and desired departure state of charge. Therefore, the owners' charging behavior should be considered in the mathematical model. The mathematical model of mobility sector can be stated as (14)-(26) Zare Oskouei & Gharehpetian [2024]. The plug-in and plug-out times as well as expected state of charge when the EVs/FCVs plug in the parking lot are known as exogenous uncertainties, which can be calculated by using the related probability distribution functions. The truncated Gaussian distribution is employed to generate scenarios depicting the initial state of charge levels of vehicles, i.e., $SOC_{(\cdot)}^{arv}$, as represented in (14). Here, μ and $\sigma_{(\cdot)}^{2}$ denote the mean value and variance of the random variable, respectively. Similarly, this function is used to generate scenarios representing the arrival and departure times of vehicles, as provided in (15) and (16). To consider the convenience of owners, the state of charge level of vehicles at the departure time must be equal to or greater than the owners' desired amount, i.e., $SOC_{(\cdot)}^{des}$, about 0.6, as stated in (17). The number of each type of EV/FCV that is available in a parking lot at a given time slot t can be calculated by (18). Constraint (19) limits the power withdrawn from (or injected back into) IEHS ($P_{t,l}^{evpl}$) to the nominal rate of charging or discharging of different types of vehicles and the number of available vehicles at the EVPLs. The maximum hydrogen charging rate of FVPLs is shown in (20). It should be noted that $H_{t,m}^{fvpl}$ is a positive variable. Constraints (21)-(23) specify how the total amount of stored energy in a parking lot ($SOE_{t,(\cdot)}$) evolves from one time period to the next. Constraint (24) represents the aggregated amount of energy added to EVPLs/FVPLs due to

the arrival of new EVs/FCVs ($SOE_{t,(\cdot)}^{arv}$); whereas, (25) refers to the total amount of reduced energy from EVPLs/FVPLs due to the end of dwell time of vehicles ($SOE_{t,(\cdot)}^{dep}$). The set of constraints (26) implies that the total state of energy (SoE) of a parking lot at each time slot should be within the state of charge level of parked vehicles.

$$SOC_{(\cdot)}^{arv} = \mathcal{G}_N\left(\chi; \mu_{SOC}, \sigma_{SOC}^2, \left(\underline{SOC_{(\cdot)}}, \overline{SOC_{(\cdot)}}\right)\right), \quad \forall (\cdot) \in \{e, f\}, \tag{14}$$

$$t_{(\cdot)}^{arv} = \mathcal{G}_{\{N/Be\}}\left(\chi; \mu_{arv}, \sigma_{arv}^2, \left(\underline{t_{(\cdot)}^{arv}}, \overline{t_{(\cdot)}^{arv}}\right)\right), \quad \forall (\cdot) \in \{e, f\}, \tag{15}$$

$$t_{(\cdot)}^{dep} = \mathcal{G}_{\{N/Be\}}\left(\chi; \mu_{dep}, \sigma_{dep}^2, \left(\underline{t_{(\cdot)}^{dep}}, \overline{t_{(\cdot)}^{dep}}\right)\right), \quad \forall (\cdot) \in \{e, f\}, \tag{16}$$

$$SOC_{(\cdot)}^{des} \le SOC_{(\cdot), t_{(\cdot)}^{dep}}^{dep}, \quad \forall (\cdot) \in \{e, f\}, \tag{17}$$

$$\omega_{t,(\cdot)} = \omega_{t-1,(\cdot)} + \omega_{t,(\cdot)}^{arv} - \omega_{t,(\cdot)}^{dep}, \quad \forall t, (\cdot) \in \{e, f\}, \tag{18}$$

$$-1 \times \sum_{e \in \mathcal{E}} \gamma_e^{dis} \omega_{t,e} \le P_{t,l}^{evpl} \le \sum_{e \in \mathcal{E}} \gamma_e^{ch} \omega_{t,e}: \quad \alpha_{t,l}^{1\uparrow}, \alpha_{t,l}^{1\downarrow}, \quad \forall t, l, \tag{19}$$

$$0 \le H_{t,m}^{fvpl} \le \sum_{f \in \mathcal{F}} \gamma_f^{ch} \omega_{t,f}: \quad \alpha_{t,m}^{2\uparrow}, \quad \forall t, m, \tag{20}$$

$$SOE_{t,l} = SOE_{t-1,l} + SOE_{t,l}^{arv} - SOE_{t,l}^{dep} + \eta\left(P_{t,l}^{evpl}\right) P_{t,l}^{evpl} \Delta t: \quad \alpha_{t,l}^3, \quad \forall t, l, \tag{21}$$

$$SOE_{t,m} = SOE_{t-1,m} + SOE_{t,m}^{arv} - SOE_{t,m}^{dep} + \eta\left(H_{t,m}^{fvpl}\right) H_{t,m}^{fvpl} \Delta t: \quad \alpha_{t,m}^4, \quad \forall t, m, \tag{22}$$

$$\eta(\cdot) = \begin{cases} \eta^{ch}: & \text{if} \quad P_{t,l}^{evpl}, H_{t,m}^{fvpl} \ge 0 \\ \eta^{dis}: & \text{if} \quad P_{t,l}^{evpl} < 0 \end{cases} \tag{23}$$

$$SOE_{t,(\cdot)}^{arv} = \sum_{(\dagger) \in \{\mathcal{E}, \mathcal{F}\}} \left(Cap_{(\dagger)} \cdot SOC_{t^{arv},(\dagger)}^{arv}\right), \quad \forall t, (\cdot) \in \{l, m\}, (\dagger) \in \{e, f\}, \tag{24}$$

$$SOE_{t,(\cdot)}^{dep} = \sum_{(\dagger) \in \{\mathcal{E}, \mathcal{F}\}} \left(Cap_{(\dagger)} \cdot SOC_{t^{dep},(\dagger)}^{dep}\right), \quad \forall t, (\cdot) \in \{l, m\}, (\dagger) \in \{e, f\}, \tag{25}$$

$$\begin{cases} \sum_{e \in \mathcal{E}} \left(\underline{SOC_e} Cap_e \omega_{t,e}\right) \le SOE_{t,l} \le \sum_{e \in \mathcal{E}} \left(\overline{SOC_e} Cap_e \omega_{t,e}\right): \quad \alpha_{t,l}^{5\uparrow}, \alpha_{t,l}^{5\downarrow} \\ \sum_{f \in \mathcal{F}} \left(\underline{SOC_f} Cap_f \omega_{t,f}\right) \le SOE_{t,m} \le \sum_{f \in \mathcal{F}} \left(\overline{SOC_f} Cap_f \omega_{t,f}\right): \quad \alpha_{t,m}^{6\uparrow}, \alpha_{t,m}^{6\downarrow} \end{cases} \tag{26}$$

In this study, the effects of human-related factors, i.e., accessibility level and probabilistic features, for the four types of most commonly used EVs and FCVs on the developed bidding/offering strategy are considered. The set of EVs types, i.e., *e1* and *e2*, are taxi and business cars; and the set of FCVs types with different pressure levels, i.e., *f1* and *f2*, are bus (450 bar) and private cars (900 bar). The scale and corresponding characteristics of the probability distribution functions of each type of vehicle are depicted in Table 2. These data are taken from reports released by the international council on clean transportation, which monitors the charging behavior of various parking lots in the United States over a 10-year period ICCT [2021].

3. Market-Oriented Operation of IEHSs

3.1. Deterministic model

The deterministic problem that describes the profit-seeking behavior of an IEHS operator, treated as a power and hydrogen prosumer, is outlined in (27). In (27), the revenue (or cost) streams arising from the participation of IEHS in the day-ahead energy as well as up/down reserve electricity markets are expressed

by γ_1-γ_3. P_t^{r+} and P_t^{r-} represent the maximum increase and decrease of power production by on-site units of the IEHS that can be requested by the independent system operator (ISO) in the regulation-up and down reserve markets, which depend on the corrective actions. Hence, term "$\lambda_t^{r+}P_t^{r+} + \lambda_t^{r-}P_t^{r-}$" represents the capacity revenues resulting from the involvement of the IEHS in the regulation-up and down reserve markets, whereas term "$\rho_t^{r+}K_t^{r+}P_t^{r+} - \rho_t^{r-}K_t^{r-}P_t^{r-}$" stands for the energy revenues in the same markets. Parameters K_t^{r+} and K_t^{r-} are in the range [0,1] and represent the fraction of non-spinning capacities of FCs, EVPLs, and electrolyzers that can be used by the IEHS operator to participate in the reserve markets. Note that, P_t^{da} is a free variable depending on the purchasing, i.e., $P_t^{da} > 0$, or selling, i.e., $P_t^{da} < 0$, power modes in the day-ahead market. γ_4 represents the earnings associated with providing power to individual consumers. γ_5 accounts for the operation cost of hydrogen storage units. Finally, γ_6 is related to the utility functions of EVs and FCVs. The defined utility functions reflect the revenue of selling power and hydrogen to EVs and FCVs for charging them, i.e., $P_{t,l}^{evpl}, H_{t,m}^{fvpl} > 0$, and the cost of buying power from EVs in discharging mode, i.e., $P_{t,l}^{evpl} < 0$, with regards to the accessibility levels of different types of vehicles, which can be calculated using (28) and (29).

$$\underset{DV}{\textbf{Max}}: \quad IEHS_{profit} = \sum_{t \in \mathcal{T}} \left[\underbrace{-P_t^{da}\lambda_t^{da}}_{\gamma_1} + \underbrace{\left(\lambda_t^{r+} + \rho_t^{r+}K_t^{r+}\right)P_t^{r+}}_{\gamma_2} + \underbrace{\left(\lambda_t^{r-} - \rho_t^{r-}K_t^{r-}\right)P_t^{r-}}_{\gamma_3} + \sum_{i \in \mathcal{I}}\underbrace{P_{t,i}^{ed}\pi_t^{re}}_{\gamma_4} - \sum_{m \in \mathcal{M}}\underbrace{\left(\rho^{fx,hs} + \rho^{va,hs}H_{t,m}^{ch}\right)}_{\gamma_5} \right] + \underbrace{\sum_{l \in \mathcal{L}}U_l + \sum_{m \in \mathcal{M}}U_m}_{\gamma_6} \tag{27}$$

$$U_l(P_l^{evpl}[\mathcal{T}], l^{th} \subset \text{Accessibility level of EVs}) = \sum_{t \in \mathcal{T}} P_{t,l}^{evpl} \cdot \pi_t^{re}, \tag{28}$$

$$U_m(H_m^{fvpl}[\mathcal{T}], m^{th} \subset \text{Accessibility level } of\ FCVs) = \sum_{t \in \mathcal{T}} H_{t,m}^{fvpl} \cdot \pi^{rh}, \tag{29}$$

The profit function, in addition to the constraints defined for the mobility sector, is also subject to the constraints of the power sector (30)-(42). Constraints (30) and (31) impose the limitations of the bidding/offering quantities in the day-ahead energy, up-reserve, and down-reserve markets, respectively. Constraint (32) ensures that the change in the output (input) power of EVPLs and FCs (electrolyzers) to participate in the regulation-up and down reserve markets does not exceed their minimum and maximum available capacity. Note that to realize the market participation model of IEHSs, the resultant generation (consumption) power of these units is $P_{t,l}^{evpl} = P_{t,l}^{evpl,da} + K_t^{r+}P_{t,l}^{evpl+} - K_t^{r-}P_{t,l}^{evpl-}$, $P_{t,m}^{fc} = P_{t,m}^{fc,da} + K_t^{r+}P_{t,m}^{fc+} - K_t^{r-}P_{t,m}^{fc-}$, and $P_{t,m}^{el} = P_{t,m}^{el,da} + K_t^{r+}P_{t,m}^{el+} - K_t^{r-}P_{t,m}^{el-}$. The day-ahead power balance of the

Table 2: Scale and probability data for different types of EVs and FCVs ICCT [2021]; Yang et al. [2020].

Vehicle types	f1:Bus (450 bar)	f2:Private car (900 bar)	e1:Taxi	e2:Business car
Major accessibility period (hour)	[22-5]	[8-17], [19-7]	[1-5]	[19-6]
$\gamma_{(\cdot)}^{dis}, \gamma_{(\cdot)}^{dis}$ rate	3 kg/min	3 kg/min	20 kW/h	6.6 kW/h
$\overline{SOC}_{(\cdot)}$ (%)		90		
$\underline{SOC}_{(\cdot)}$ (%)		30		
Capacity	12 kg	6 kg	100 kWh	40 kWh
$(\mu_{SOC^{arv}}, \sigma_{SOC}^2)$	N(0.5, 0.003)	N(0.5, 0.003)	N(0.4, 0.002)	N(0.4, 0.002)
$(\mu_{SOC^{dep}}, \sigma_{SOC}^2)$		N(0.7, 0.003)		
$(\mu_{t^{arv}}, \sigma_{t^{arv}}^2)$	N(1, 3)	N(10, 3), N(22, 3)	N(2, 2)	N(20, 2)
$(\mu_{t^{dep}}, \sigma_{t^{dep}}^2)$	N(6, 3)	N(19, 2), N(9, 2)	N(8, 3)	N(7, 3)

IEHS is given by (33) and (34), which integrates power injections from on-site units located in IEHS and power drawn by individual consumers and EVs at each bus. The proposed model integrates the first-order Taylor expansion and polyhedral programming relaxation approaches to turn the original non-linear and non-convex AC power flow problem into a convex optimization model and a tractable linear problem Zare Oskouei et al. [2022], which can be guaranteed the global optimality of the solutions. The piecewise linearized AC power flow model is represented by (35)-(39). Here, $\widetilde{cos}\left(\theta_{ij,t}\right)$ denotes the polyhedral relaxation of $cos\left(\theta_{ij,t}\right)$. It should be noted that in (37), the sine and cosine functions are defined for set $\mathcal{D}$ and do not have a fixed value, and the size of this set can affect the accuracy of linearization of the AC power flow model. This linearization is primarily based on the formulation of Akbari & Tavakoli Bina [2016]; Coffrin & Van Hentenryck [2014]. The voltage magnitude and angle at each bus should be restricted to upper and lower limits, as provided in (40) and (41). Finally, (42) ensures that the wind power dispatch at each time slot does not exceed WFs allowable range.

$$-\overline{P^{da}} \leq P_t^{da} \leq \overline{P^{da}}, \quad \forall t, \tag{30}$$

$$\begin{cases} 0 \leq P_t^{r+} = \sum_{l\in\mathcal{L}} P_{t,l}^{evpl+} + \sum_{m\in\Theta_i^{\mathcal{M}}} \left(P_{t,m}^{fc+} + P_{t,m}^{el+}\right) \leq \overline{P^{r+}} \\ 0 \leq P_t^{r-} = \sum_{l\in\mathcal{L}} P_{t,l}^{evpl-} + \sum_{m\in\Theta_i^{\mathcal{M}}} \left(P_{t,m}^{fc-} + P_{t,m}^{el-}\right) \leq \overline{P^{r-}} \end{cases} \tag{31}$$

$$\begin{cases} 0 \leq P_{t,l}^{evpl+} \leq \underline{SoE_{t,l}} + P_{t,l}^{evpl,da}, 0 \leq P_{t,l}^{evpl-} \leq \overline{SoE_{t,l}} - P_{t,l}^{evpl,da} \\ 0 \leq P_{t,m}^{fc+} \leq \overline{P_m^{fc}} - P_{t,m}^{fc,da}, \qquad 0 \leq P_{t,m}^{fc-} \leq P_{t,m}^{fc,da} \\ 0 \leq P_{t,m}^{el+} \leq P_{t,m}^{el,da}, \qquad 0 \leq P_{t,m}^{el-} \leq \overline{P_m^{el}} - P_{t,m}^{el,da} \end{cases} \tag{32}$$

$$\left(P_t^{da} - K_t^{r+}P_t^{r+} + K_t^{r-}P_t^{r-}\right)\Big|_{i\in pcc} + P_{t,i}^{w,da} - P_{t,i}^{ed} - \sum_{l\in\Theta_i^{\mathcal{L}}} P_{t,l}^{evpl} + \sum_{m\in\Theta_i^{\mathcal{M}}} \left(P_{t,m}^{fc} - P_{t,m}^{el}\right) = \sum_{j,(i,j)\in\mathcal{K}} FL_{t,ij} : \quad \partial_{t,i}^1,$$

$$\forall t, i, \tag{33}$$

$$\left(Q_t^{da} - \beta^{pf}\left(K_t^{r+}P_t^{r+} - K_t^{r-}P_t^{r-}\right)\right)\Big|_{i\in pcc} - Q_{t,i}^{ed} + \beta^{pf,w}P_{t,i}^{w,da} = \sum_{j,(i,j)\in\mathcal{K}} \widetilde{FL}_{t,ij} : \quad \partial_{t,i}^2, \quad \forall t, i, \tag{34}$$

$$\frac{FL_{t,ij}}{S_{base}} \approx g_{ij}\left(V_{t,i} - V_{t,j} - \widetilde{cos}\left(\theta_{t,ij}\right) + 1\right) - b_{ij}\theta_{t,ij}, \forall t, (i,j) \in \mathcal{K}, \tag{35}$$

$$\frac{\widetilde{FL}_{t,ij}}{S_{base}} \approx -b_{ij}\left(V_{i,t} - V_{j,t} - \widetilde{cos}\left(\theta_{ij,t}\right) + 1\right) - g_{ij}\theta_{ij,t}, \forall t, (i,j), \tag{36}$$

$$\left[\sin\left(\frac{2\pi\mathcal{D}}{d}\right) - \sin\left(\frac{2\pi(\mathcal{D}-1)}{d}\right)\right] FL_{t,ij} - \left[\cos\left(\frac{2\pi\mathcal{D}}{d}\right) - \cos\left(\frac{2\pi(\mathcal{D}-1)}{d}\right)\right] \widetilde{FL}_{t,ij} - \left|\overline{SL_{ij}}\right|\sin\left(\frac{2\pi}{d}\right) \leq 0 : \quad \zeta_{t,i,j},$$

$$\forall \mathcal{D} \in \{1, 2, \ldots, d\}, t, (i,j) \in \mathcal{K}, \tag{37}$$

$$-\left|\overline{SL_{ij}}\right| \leq FL_{t,ij} \leq \left|\overline{SL_{ij}}\right| : \quad \zeta_{t,i,j}^{1\uparrow}, \zeta_{t,i,j}^{1\downarrow}, \quad \forall t, (i,j) \in \mathcal{K}, \tag{38}$$

$$-\left|\overline{SL_{ij}}\right| \leq \widetilde{FL}_{t,ij} \leq \left|\overline{SL_{ij}}\right| : \quad \zeta_{t,i,j}^{2\uparrow}, \zeta_{t,i,j}^{2\downarrow}, \quad \forall t, (i,j) \in \mathcal{K}, \tag{39}$$

$$\underline{V_i} \leq V_{t,i} \leq \overline{V}_i : \quad \tau_{t,i}^{\uparrow}, \tau_{t,i}^{\downarrow}, \quad \forall t, i, \tag{40}$$

$$-\pi \leq \theta_{t,ij} \leq \pi : \quad \tau'^{\downarrow}_{t,i}, \tau'^{\uparrow}_{t,ij}, \quad \forall t,i,j, \tag{41}$$

$$0 \leq P^{w,da}_{t,i} \leq P^{w,f}_{t,i} : \quad \sigma_{t,i}, \quad \forall t,i. \tag{42}$$

3.2. Characterization of uncertainty

To assess the risk of profit variability encountered by the uncertainties of wind power generation, electricity market prices, and calls for reserve service, the presented deterministic bidding/offering strategy is developed as the tri-level stochastic adaptive robust optimization approach. Since the variation in electricity market prices does not pose a problem with the power quality of IEHS, therefore, such uncertainty sources must be treated as *soft constraints*. Hence, the uncertainty of electricity market prices is described by the stochastic programming framework, which uses Monte Carlo Simulation to generate the finite discrete random scenarios with their corresponding probabilities, denoted by $\lambda^{da}_{t,s}$, $\rho^{r+}_{t,s}$, and $\rho^{r-}_{t,s}$.

On the other hand, erroneous predictions of the wind power production level and calls for reserve service may affect the quality of service, therefore, these uncertain parameters must be treated as *hard constraints*. Hence, continuous uncertainty sets, i.e., Δ, in the context of the adaptive robust optimization method are employed to handle the randomness of such hard constraints, which can be described as (43)-(48). The available wind power production is stated in terms of the fluctuation, i.e., $z^{w\uparrow}_{t,i} \widehat{P^w_{t,i}}$ or $z^{w\downarrow}_{t,i} \widehat{P^w_{t,i}}$, and average, i.e., $\widetilde{P^w_{t,i}}$, levels associated with the respective confidence limits, as provided in (44). Constraint (47) ensures that ISO cannot simultaneously request to supply both downward and upward reserves. Γ^w and Γ^r serve as a budget to characterize the worst-case available wind power generation and the worst-case reserve deployment requests, that can take values between 0 and $\mathcal{T}$. In other words, these positive parameters are used to model the tradeoff between uncertainty immunization and expected profit based on the conservatism level of the IEHS operator. Constraints (46) and (48) address the conservativeness of the strategy through the wind uncertainty budget and the reserve uncertainty budget.

$$\Delta = \Big\{ \Phi^{ML} : z^{w\uparrow}_{t,i}, z^{w\downarrow}_{t,i}, \nu^{r+}_t, \nu^{r-}_t \in \{0,1\}, \quad \forall t, \tag{43}$$

$$P^{w,f}_{t,i} = \widetilde{P^w_{t,i}} + z^{w\uparrow}_{t,i} \widehat{P^w_{t,i}} - z^{w\downarrow}_{t,i} \widehat{P^w_{t,i}}, \quad \forall t,i, \tag{44}$$

$$z^{w\uparrow}_{t,i} + z^{w\downarrow}_{t,i} \leq 1, \quad \forall t,i, \tag{45}$$

$$\sum_{t \in \mathcal{T}} \sum_{i \in \mathcal{I}} \left(z^{w\uparrow}_{t,i} + z^{w\downarrow}_{t,i} \right) \leq \Gamma^w, \tag{46}$$

$$\nu^{r+}_t + \nu^{r-}_t \leq 1, \quad \forall t, \tag{47}$$

$$\sum_{t \in \mathcal{T}} \left(\nu^{r+}_t + \nu^{r-}_t \right) \leq \Gamma^r. \Big\} \tag{48}$$

3.3. Stochastic adaptive robust scheduling model

The developed tri-level stochastic adaptive robust formulation for the bidding/offering problem of IEHSs is manifested in (49), subject to (50). The upper-level is related to the day-ahead energy and reserve market decisions to maximize the worst-case expected profit of the IEHS. The set of upper-level decision variables involved in the scheduling is $\Phi^{UL} = \left\{ P_t^{da}, P_t^{r+}, P_t^{r-} \right\}$. By determining the upper-level decision vector, the middle-level identifies the worst-case realization of reserve deployment calls and wind power production to minimize the expected profit of the IEHS. The decision variables related to this level are $\Phi^{ML} = \left\{ z_{t,i}^{w\uparrow}, z_{t,i}^{w\downarrow}, \nu_t^{r+}, \nu_t^{r-}, P_{t,i}^{w,f} \right\}$. The lower-level tries to maximize the expected profit of the IEHS in response to upper- and middle-level decisions according to the defined decision variables, i.e., $\Phi^{LL} = \left\{ P_{t,i}^{w,da}, V_{t,i}, \theta_{t,ij}, FL_{t,ij}, \widetilde{FL}_{t,ij}, P_{t,l}^{evpl}, H_{t,m}^{fvpl}, P_{t,m}^{fc}, H_{t,m}^{fc}, SOE_{t,l}, SOE_{t,m}, H_{t,m}^{ch}, H_{t,m}^{dis}, SOC_{t,m}^{hs}, P_{t,m}^{el}, H_{t,m}^{gen}, P_{t,m}^{ie}, P_{t,m}^{com}, H_{t,m}^{sv}, H_{t,m}^{elv} \right\}$. It should be noted that, all defined variables must be indexed by "s", meaning they must hold for each scenario.

$$IEHS_{profit} =$$

$$\underset{\Phi^{UL}}{\textbf{Max}} \sum_{s \in \mathcal{S}} \Omega_s \left[\sum_{t \in \mathcal{T}} \left(-\lambda_{t,s}^{da} P_t^{da} + \lambda_t^{r+} P_t^{r+} + \lambda_t^{r-} P_t^{r-} + \sum_{i \in \mathcal{I}} P_{t,i}^{ed} \pi_t^{re} \right) \right] +$$

$$\underset{\Phi^{ML} \in \Delta}{\textbf{Min}} \underset{\Phi^{LL} \in \Psi}{\textbf{Max}} \sum_{s \in \mathcal{S}} \Omega_s \left[\sum_{t \in \mathcal{T}} \left(\rho_{t,s}^{r+} \nu_t^{r+} K_t^{r+} P_t^{r+} - \rho_{t,s}^{r-} \nu_t^{r-} K_t^{r-} P_t^{r-} \right. \right. \tag{49}$$

$$\left. \left. - \sum_{m \in \mathcal{M}} \left(\rho^{fx,hs} + \rho^{va,hs} H_{t,m}^{ch} \right) \right) + \sum_{l \in \mathcal{L}} U_l + \sum_{m \in \mathcal{M}} U_m \right]$$

subject to:

$$(28) - (32) \tag{50}$$

Ψ is defined as the feasibility set to determine the feasible space of lower-level optimization variables according to the upper-level and middle-level optimization variables, as described in (51).

$$\Psi = \left\{ \Phi^{LL} : (1) - (26), (33) - (42) \right\} \tag{51}$$

4. Solution Procedure

To solve the developed stochastic adaptive robust optimization problem (49), the nested column-and-constraint generation (C&CG) algorithm Baringo & Baringo [2017] is adopted, which decomposes the original problem into a master problem and a sub-problem. This algorithm solves the master problem and sub-problem in an iterative manner until convergence to an optimal solution.

4.1. Master problem

Suppose that the χ'^{th} iteration is the developed optimization problem. Let $\nu_t^{r+(\chi)}$, $\nu_t^{r-(\chi)}$, and $P_{t,i}^{w,f(\chi)}$ denote the optimal solution of ν_t^{r+}, ν_t^{r-}, and $P_{t,i}^{w,f}$ that are yielded by sub-problem at a prior iteration $(\chi'-1)^{th}$. The master problem associated with original model (49) is provided as (52)-(58). The optimal objective value of (52), i.e., z^{MP*}, provides an upper bound on the optimal objective value of the original model at each iteration. Simply put, the master problem is a relaxed state of the original problem (49) that uses the auxiliary variable δ to approximate the worst value of the middle-level objective function at iteration χ'^{th}.

$$\underset{\Phi^{UL'}}{\textbf{Max}} \sum_{s \in \mathcal{S}} \Omega_s \left[\sum_{t \in \mathcal{T}} \left(-\lambda_{t,s}^{da} P_t^{da} + \lambda_t^{r+} P_t^{r+} + \lambda_t^{r-} P_t^{r-} + \sum_{i \in \mathcal{I}} P_{t,i}^{ed} \pi_t^{re} \right) \right] + \delta \tag{52}$$

subject to:

$$(30) - (32) \tag{53}$$

$$
\begin{aligned}
\delta \leq \sum_{s \in \mathcal{S}} \Omega_s \Bigg[&\sum_{t \in \mathcal{T}} \Big(\rho_{t,s}^{r+} \nu_t^{r+(\chi)} K_t^{r+} P_t^{r+} - \rho_{t,s}^{r-} \nu_t^{r-(\chi)} K_t^{r-} P_t^{r-} \\
&- \sum_{m \in \mathcal{M}} \Big(\rho^{fx,hs} + \rho^{va,hs} H_{t,m,\chi'}^{ch} \Big) + \sum_{l \in \mathcal{L}} P_{t,l,\chi'}^{evpl} \pi_t^{re} + \sum_{m \in \mathcal{M}} H_{t,m,\chi'}^{fvpl} \pi^{rh} \Big) \Bigg], \quad \forall \chi' = 1, ..., \chi,
\end{aligned}
\tag{54}
$$

$$
\begin{aligned}
\Big(P_t^{da} - \nu_t^{r+(\chi)} K_t^{r+} P_t^{r+} + \nu_t^{r-(\chi)} K_t^{r-} P_t^{r-} \Big) \Big|_{i \in pcc} + P_{t,i,\chi'}^{w,da} - P_{t,i}^{ed} - \\
\sum_{l \in \Theta_i^{\mathcal{L}}} P_{t,l,\chi'}^{evpl} + \sum_{m \in \Theta_i^{\mathcal{M}}} \Big(P_{t,m,\chi'}^{fc} - P_{t,m,\chi'}^{el} \Big) = \sum_{j,(i,j) \in \mathcal{K}} FL_{t,ij,\chi'}, \quad \forall t,i,\chi',
\end{aligned}
\tag{55}
$$

$$
\beta^{pf} \Big(P_t^{da} - \nu_t^{r+(\chi)} K_t^{r+} P_t^{r+} + \nu_t^{r-(\chi)} K_t^{r-} P_t^{r-} \Big) \Big|_{i \in pcc} - Q_{t,i}^{ed} + \beta^{pf,w} P_{t,i,\chi'}^{w,da} = \sum_{j,(i,j) \in \mathcal{K}} \widetilde{FL}_{t,ij,\chi'}, \quad \forall t,i,\chi', \tag{56}
$$

$$
0 \leq P_{t,i,\chi'}^{w,da} \leq P_{t,i}^{w,f(\chi)}, \quad \forall t,i,\chi', \tag{57}
$$

$$
\begin{aligned}
(1) - (13) \\
(19) - (22), (26) \\
(35) - (41)
\end{aligned}
\left|
\begin{aligned}
&V_{t,i} \to V_{t,i,\chi'}, \theta_{t,ij} \to \theta_{t,ij,\chi'}, \\
&FL_{t,ij} \to FL_{t,ij,\chi'}, \widetilde{FL}_{t,ij} \to \widetilde{FL}_{t,ij,\chi'}, \\
&P_{t,l}^{evpl} \to P_{t,l,\chi'}^{evpl}, H_{t,m}^{fvpl} \to H_{t,m,\chi'}^{fvpl}, \\
&SOE_{t,l} \to SOE_{t,l,\chi'}, SOE_{t,m} \to SOE_{t,m,\chi'}, \\
&H_{t,m}^{ch} \to H_{t,m,\chi'}^{ch}, H_{t,m}^{dis} \to H_{t,m,\chi'}^{dis}, \\
&SOC_{t,m}^{hs} \to SOC_{t,m,\chi'}^{hs}, P_{t,m}^{fc} \to P_{t,m,\chi'}^{fc}, \\
&H_{t,m}^{fc} \to H_{t,m,\chi'}^{fc}, H_{t,m}^{gen} \to H_{t,m,\chi'}^{gen}, \\
&P_{t,m}^{el} \to P_{t,m,\chi'}^{el}, P_{t,m}^{com} \to P_{t,m,\chi'}^{com}, \\
&P_{t,m}^{ie} \to P_{t,m,\chi'}^{ie}, H_{t,m}^{sv} \to H_{t,m,\chi'}^{sv}, \\
&H_{t,m}^{elv} \to H_{t,m,\chi'}^{elv}, \\
\\
&\forall t,i,e,f,m,l,\chi'.
\end{aligned}
\right. \tag{58}
$$

$$
\begin{aligned}
\Phi^{UL'} = \{ \Phi^{UL} \} \cup \{ &\delta, P_{t,i,\chi'}^{w}, V_{t,i,\chi'}, \theta_{t,ij,\chi'}, FL_{t,ij,\chi'}, \widetilde{FL}_{t,ij,\chi'}, P_{t,l,\chi'}^{evpl}, H_{t,m,\chi'}^{fvpl}, SOE_{t,l,\chi'}, SOE_{t,m,\chi'}, H_{t,m,\chi'}^{ch}, H_{t,m,\chi'}^{dis}, \\
&SOC_{t,m,\chi'}^{hs}, P_{t,m,\chi'}^{fc}, H_{t,m,\chi'}^{fc}, P_{t,m,\chi'}^{el}, H_{t,m,\chi'}^{gen}, P_{t,m,\chi'}^{ie}, P_{t,m,\chi'}^{com}, H_{t,m,\chi'}^{sv}, H_{t,m,\chi'}^{elv} \}
\end{aligned}
$$

4.2. Sub-problem

The sub-problem at each iteration χ' is cast as (59)-(62). Since the master problem is solved prior to the sub-problem, variables $P_t^{da(\chi)}$, $P_t^{r+(\chi)}$, and $P_t^{r-(\chi)}$ are fixed at their optimal values obtained from the master problem. The day-ahead power balance restrictions, i.e., (60) and (61), are relaxed with two non-negative slack variables y_t^+ and y_t^-, which are penalized in (59) using a cost coefficient, i.e., $\mathscr{B} > 0$, to ensure the feasibility of the sub-problem throughout the iterative process.

$$
\begin{aligned}
\min_{\Phi^{ML} \in \Delta} \max_{\Phi^{LL'}} \sum_{s \in \mathcal{S}} \Omega_s \Bigg[&\sum_{t \in \mathcal{T}} \Big(\rho_{t,s}^{r+} \nu_t^{r+} K_t^{r+} P_t^{r+(\chi)} - \rho_{t,s}^{r-} \nu_t^{r-} K_t^{r-} P_t^{r-(\chi)} \\
&- \sum_{m \in \mathcal{M}} \Big(\rho^{fx,hs} + \rho^{va,hs} H_{t,m}^{ch} \Big) + \sum_{l \in \mathcal{L}} P_{t,l}^{evpl} \pi_t^{re} + \sum_{m \in \mathcal{M}} H_{t,m}^{fvpl} \pi^{rh} \Big) - \mathscr{B}(y_t^+ + y_t^-) \Bigg]
\end{aligned}
\tag{59}
$$

subject to:

$$\left(P_t^{da(\chi)} - \nu_t^{r+} K_t^{r+} P_t^{r+(\chi)} + \nu_t^{r-} K_t^{r-} P_t^{r-(\chi)}\right)\Big|_{i\in pcc} + P_{t,i}^{w,da} - P_{t,i}^{ed} -$$
$$\sum_{l\in\Theta_i^{\mathcal{L}}} P_{t,l}^{evpl} + \sum_{m\in\Theta_i^{\mathcal{M}}} \left(P_{t,m}^{fc} - P_{t,m}^{el}\right) + y_t^+ - y_t^- = \sum_{j,(i,j)\in\mathcal{K}} FL_{t,ij}: \quad \partial_{t,i}^1, \quad \forall t,i, \tag{60}$$

$$\beta^{pf}\left(P_t^{da(\chi)} - \nu_t^{r+} K_t^{r+} P_t^{r+(\chi)} + \nu_t^{r-} K_t^{r-} P_t^{r-(\chi)}\right)\Big|_{i\in pcc} - Q_{t,i}^{ed} + \beta^{pf,w} P_{t,i}^{w,da} + y_t^+ - y_t^- = \sum_{j,(i,j)\in\mathcal{K}} \widetilde{FL}_{t,ij}: \quad \partial_{t,i}^2, \tag{61}$$

$$(1) - (26), (35) - (42) \tag{62}$$

where $\Phi^{LL'} = \left\{\Phi^{LL}\right\} \cup \left\{y_t^+, y_t^-\right\}$.

Since the sub-problem is linear and continuous in its decision variables, accordingly, the internal maximization problem can be replaced with the equivalent dual optimization problem using KKT conditions rendering the single-level minimization problem, as stated in (63)-(88).

$$\underset{\Phi^{DS}}{\mathbf{Min}} \sum_s \Omega_s \Bigg[\sum_t \left(\rho_{t,s}^{r+}\nu_t^{r+} K_t^{r+} P_t^{r+(\chi)} - \rho_{t,s}^{r-}\nu_t^{r-} K_t^{r-} P_t^{r-(\chi)}\right) - \Bigg[\sum_t \Bigg[\sum_{i,j}\left(\left(\partial_{t,i}^1\left(-P_{t,1}^{da(\chi)} + \nu_t^{r+} K_t^{r+} P_{t,1}^{r+(\chi)} - \nu_t^{r-} K_t^{r-} P_{t,1}^{r-(\chi)}\right)\right.\right.$$
$$\left.+ P_{t,i}^{ed} + S_{base}g_{ij}\right) - \partial_{t,i}^2 \beta^{pf}\left(P_{t,1}^{da(\chi)} - \nu_t^{r+} K_t^{r+} P_{t,1}^{r+(\chi)} + \nu_t^{r-} K_t^{r-} P_{t,1}^{r-(\chi)} + Q_{t,i}^{ed} - S_{base}b_{ij}\right) + \tau_{t,i}^\uparrow \overline{V}_i - \tau_{t,i}^\downarrow \underline{V_i} + \sigma_{t,i} P_{t,i}^{w,f}$$
$$+ \zeta_{t,i,j}^{1\uparrow}\left(\left|\overline{SL_{ij}}\right| - S_{base}g_{ij}\right) + \zeta_{t,i,j}^{1\downarrow}\left(\left|\overline{SL_{ij}}\right| + S_{base}g_{ij}\right) + \zeta_{t,i,j}^{2\uparrow}\left(\left|\overline{SL_{ij}}\right| + S_{base}b_{ij}\right) + \zeta_{t,i,j}^{2\downarrow}\left(\left|\overline{SL_{ij}}\right| - S_{base}b_{ij}\right) +$$
$$\pi\left(\tau_{t,ij}'^\uparrow - \tau_{t,ij}'^\downarrow\right)\right) + \sum_{i,j,d} \zeta_{t,i,j}\left(\left|\overline{SL_{ij}}\right|\sin\left(\frac{2\pi}{d}\right) - S_{base}g_{ij}\left(\sin\left(\frac{2\pi D}{d}\right) - \sin\left(\frac{2\pi(D-1)}{d}\right)\right) - S_{base}b_{ij}\left(\cos\left(\frac{2\pi D}{d}\right) - \cos\left(\frac{2\pi(D-1)}{d}\right)\right)\right) +$$
$$\sum_{l,e}\left(\alpha_{t,l}^{1\uparrow}\gamma_e^{ch}\omega_{t,e} + \alpha_{t,l}^{1\downarrow}\gamma_e^{dis}\omega_{t,e} + \alpha_{t,l}^3\left(SOE_{0,l} + SOE_{t,l}^{arv} - SOE_{t,l}^{dep}\right) + \alpha_{t,l}^{5\uparrow}\overline{SOC_e}Cap_e\omega_{t,e} - \alpha_{t,l}^{5\downarrow}\underline{SOC_e}Cap_e\omega_{t,e}\right) +$$
$$\sum_{m,f}\left(\alpha_{t,m}^{2\uparrow}\gamma_f^{ch}\omega_{t,f} + \alpha_{t,m}^{6\uparrow}\overline{SOC_f}Cap_f\omega_{t,f} - \alpha_{t,m}^{6\downarrow}\underline{SOC_f}Cap_f\omega_{t,f} + \alpha_{t,m}^4\left(SOE_{0,m} + SOE_{t,m}^{arv} - SOE_{t,m}^{dep}\right)\right) +$$
$$\sum_m\left(\gamma_{1,m}^4 0.95SOC_{0,m}^{hs} + \gamma_{t,m}^{8\uparrow}\overline{H^{gen}} - \gamma_{t,m}^{8\downarrow}\underline{H^{gen}} + \gamma_{t,m}^{9\uparrow}\overline{H^{fc}} - \gamma_{t,m}^{9\downarrow}\underline{H^{fc}} + \gamma_{t,m}^{10\uparrow}\overline{SOC^{hs}} - \gamma_{t,m}^{10\downarrow}\underline{SOC^{hs}} + \gamma_{t,m}^{11\uparrow}\overline{H^{ch}} + \gamma_{t,m}^{12\uparrow}\overline{H^{dis}}\right)\Bigg]\Bigg]\Bigg] \tag{63}$$

subject to:

$$(43) - (48) \tag{64}$$

$$\partial_{t,i}^1 + \partial_{t,i}^2 \geq \mathscr{B}, \quad \forall t,i, \tag{65}$$

$$-\partial_{t,i}^1 - \partial_{t,i}^2 \geq \mathscr{B}, \quad \forall t,i, \tag{66}$$

$$\partial_{t,i}^1 + \beta^{pf,w}\partial_{t,i}^2 + \sigma_{t,i} \geq 0, \quad \forall t,i, \tag{67}$$

$$S_{base}\left(b_{ij}\partial_{t,i}^2 - g_{ij}\partial_{t,i}^1\right) + \tau_{t,i}^\uparrow - \tau_{t,i}^\downarrow + \zeta_{t,i,j}S_{base}g_{ij}\left[\sin\left(\frac{2\pi D}{d}\right) - \sin\left(\frac{2\pi(D-1)}{d}\right)\right] + \zeta_{t,i,j}S_{base}b_{ij}\left[\cos\left(\frac{2\pi D}{d}\right) - \cos\left(\frac{2\pi(D-1)}{d}\right)\right]$$
$$+ \left(\zeta_{t,i,j}^{1\uparrow} - \zeta_{t,i,j}^{1\downarrow}\right)S_{base}g_{ij} + S_{base}b_{ij}\left(\zeta_{t,i,j}^{2\downarrow} - \zeta_{t,i,j}^{2\uparrow}\right) \geq 0, \quad \forall t,i,j,d, \tag{68}$$

$$S_{base}\left(b_{ij}\partial_{t,i}^1 + g_{ij}\partial_{t,i}^2\right) + \tau_{t,i}'^\uparrow - \tau_{t,i}'^\downarrow - \zeta_{t,i,j}S_{base}b_{ij}\left[\sin\left(\frac{2\pi D}{d}\right) - \sin\left(\frac{2\pi(D-1)}{d}\right)\right] +$$
$$\zeta_{t,i,j}S_{base}g_{ij}\left[\cos\left(\frac{2\pi D}{d}\right) - \cos\left(\frac{2\pi(D-1)}{d}\right)\right] + \left(\zeta_{t,i,j}^{1\downarrow} - \zeta_{t,i,j}^{1\uparrow}\right)S_{base}b_{ij} + S_{base}g_{ij}\left(\zeta_{t,i,j}^{2\downarrow} - \zeta_{t,i,j}^{2\uparrow}\right) = 0, \tag{69}$$

$$-\partial_{t,i}^1 + \alpha_{t,l}^{1\uparrow} - \alpha_{t,l}^{1\downarrow} - \eta\left(P_{t,l}^{evpl}\right)\Delta t\alpha_{t,l}^3 = -\pi_t^{re}, \quad \forall t,i,l, \tag{70}$$

$$\alpha_{t,m}^{2\uparrow} - \eta^{ch}\Delta t\alpha_{t,m}^4 = -\pi^{rh}, \quad \forall t,m, \tag{71}$$

19

$$\alpha_{t,l}^3 + \alpha_{t,l}^{5\uparrow} - \alpha_{t,l}^{5\downarrow} - \alpha_{t+1,l}^3 \geq 0, \quad \forall t = 1, ..., \mathcal{T} - 1, l, \tag{72}$$

$$\alpha_{\mathcal{T},l}^3 + \alpha_{\mathcal{T},l}^{5\uparrow} - \alpha_{\mathcal{T},l}^{5\downarrow} \geq 0, \quad \forall l, \tag{73}$$

$$\alpha_{t,m}^4 + \alpha_{t,m}^{6\uparrow} - \alpha_{t,m}^{6\downarrow} - \alpha_{t+1,m}^4 \geq 0, \quad \forall t = 1, ..., \mathcal{T} - 1, m, \tag{74}$$

$$\alpha_{\mathcal{T},m}^4 + \alpha_{\mathcal{T},m}^{6\uparrow} - \alpha_{\mathcal{T},m}^{6\downarrow} \geq 0, \quad \forall m, \tag{75}$$

$$\gamma_{t,m}^3 - \gamma_{t,m}^4 \frac{\eta^{ch}\Delta t}{Cap^{hs}} + \gamma_{t,m}^{11\uparrow} \geq \rho^{va,hs}, \quad \forall t, m, \tag{76}$$

$$\gamma_{t,m}^4 \frac{\Delta t}{\eta^{dis}Cap^{hs}} - \gamma_{t,m}^5 + \gamma_{t,m}^{12\uparrow} \geq 0, \quad \forall t, m, \tag{77}$$

$$\gamma_{t,m}^4 + \gamma_{t,m}^{10\uparrow} - \gamma_{t,m}^{10\downarrow} - \gamma_{t+1,m}^4 \geq 0, \quad \forall t = 1, ..., \mathcal{T} - 1, m, \tag{78}$$

$$\gamma_{\mathcal{T},m}^4 + \gamma_{\mathcal{T},m}^{10\uparrow} - \gamma_{\mathcal{T},m}^{10\downarrow} \geq 0, \quad \forall m, \tag{79}$$

$$\partial_{t,i}^1 - \gamma_{t,m}^7 \geq 0, \quad \forall t, m, i, \tag{80}$$

$$\gamma_{t,m}^5 + \kappa^{H2E}\gamma_{t,m}^7 + \gamma_{t,m}^{9\uparrow} - \gamma_{t,m}^{9\downarrow} \geq 0, \quad \forall t, m, \tag{81}$$

$$-\partial_{t,i}^1 - \gamma_{t,m}^2 + \gamma_{t,m}^{8\uparrow} - \gamma_{t,m}^{8\downarrow} \geq 0, \quad \forall t, m, i, \tag{82}$$

$$-\frac{\gamma_{t,m}^1}{\kappa^{H2C}} + \gamma_{t,m}^2 - \frac{\gamma_{t,m}^3}{\kappa^{H2C}} \geq 0, \quad \forall t, m, \tag{83}$$

$$\kappa^{E2H}\gamma_{t,m}^1 + \gamma_{t,m}^2 \geq 0, \quad \forall t, m, \tag{84}$$

$$\gamma_{t,m}^5 + \gamma_{t,m}^6 = 0, \quad \forall t, m, \tag{85}$$

$$\gamma_{t,m}^3 + \gamma_{t,m}^6 = 0, \quad \forall t, m, \tag{86}$$

$$\tau_{t,i}^\uparrow, \tau_{t,i}^\downarrow, \tau'^\uparrow_{t,ij}, \tau'^\downarrow_{t,ij}, \sigma_{t,i}, \zeta_{t,i,j}, \zeta_{t,i,j}^{1\uparrow}, \zeta_{t,i,j}^{1\downarrow}, \zeta_{t,i,j}^{2\uparrow}, \zeta_{t,i,j}^{2\downarrow}, \alpha_{t,l}^{1\uparrow}, \alpha_{t,l}^{1\downarrow}, \alpha_{t,m}^{2\uparrow}, \alpha_{t,m}^{2\downarrow}, \alpha_{t,l}^{5\uparrow}, \alpha_{t,l}^{5\downarrow}, \alpha_{t,m}^{6\uparrow}, \alpha_{t,m}^{6\downarrow}, \gamma_{t,m}^{8\uparrow}, \gamma_{t,m}^{8\downarrow},$$
$$\gamma_{t,m}^{9\uparrow}, \gamma_{t,m}^{9\downarrow}, \gamma_{t,m}^{10\uparrow}, \gamma_{t,m}^{10\downarrow}, \gamma_{t,m}^{11\uparrow}, \gamma_{t,m}^{12\uparrow} \geq 0, \quad \forall t, i, l, m \tag{87}$$

$$\partial_{t,i}^1, \partial_{t,i}^2, \alpha_{t,l}^3, \alpha_{t,m}^4, \gamma_{t,m}^1 - \gamma_{t,m}^7 \in \mathcal{R}, \quad \forall t, i, l, m. \tag{88}$$

After obtaining the dual minimization problem, $\partial_{t,i}^1 \nu_t^{r+} P_{t,1}^{r+(\chi)}$, $\partial_{t,i}^1 \nu_t^{r-} P_{t,1}^{r-(\chi)}$, $\partial_{t,i}^2 \nu_t^{r+} P_{t,1}^{r+(\chi)}$, $\partial_{t,i}^2 \nu_t^{r-} P_{t,1}^{r-(\chi)}$, and $\sigma_{t,i} P_{t,i}^{w,f}$ are recognized as the non-linear terms in the context of the middle-level variables and the lower-level dual variables. According to defined uncertainty set, the term "$\sigma_{t,i} P_{t,i}^{w,f}$" is equal to "$\sigma_{t,i}\widetilde{P_{t,i}^w} + \sigma_{t,i}z_{t,i}^{w\uparrow}\widehat{P_{t,i}^w} - \sigma_{t,i}z_{t,i}^{w\downarrow}\widehat{P_{t,i}^w}$", thereby giving rise to additional bilinear terms, i.e., "$\sigma_{t,i}z_{t,i}^{w\uparrow}\widehat{P_{t,i}^w}$" and "$\sigma_{t,i}z_{t,i}^{w\downarrow}\widehat{P_{t,i}^w}$". According to the linearization scheme described in Floudas [1995], a linear equivalent can be defined for the product of a continues variable P, i.e., $P \in [\overline{P}, \underline{P}]$, and a binary variable q, i.e., $q \in \{0, 1\}$. To this end, a new continuous variable X should be defined and replaced with the product $P \cdot q$. After that, restrictions (89) and (90) can be used to linearize the term "$P \cdot q$".

$$\underline{P} \cdot q \leq X \leq \overline{P} \cdot q \tag{89}$$

$$\underline{P} \cdot (1 - q) \leq P - X \leq \overline{P} \cdot (1 - q) \tag{90}$$

According to this definition, we must define six continuous variables, which are presented in (91), and then we have to replace the existing bilinear terms with related linear restrictions, which leads to adding twelve constraints to the dual sub-problem.

$$
\begin{cases}
\partial_{t,i}^1 \nu_t^{r+} = X_{t,i}^{r1+} \\
\partial_{t,i}^1 \nu_t^{r-} = X_{t,i}^{r1-} \\
\partial_{t,i}^2 \nu_t^{r+} = X_{t,i}^{r2+}
\end{cases}
\qquad
\begin{cases}
\partial_{t,i}^2 \nu_t^{r-} = X_{t,i}^{r2-} \\
\sigma_{t,i} z_{t,i}^{w\uparrow} = X_{t,i}^{w\uparrow} \\
\sigma_{t,i} z_{t,i}^{w\downarrow} = X_{t,i}^{w\downarrow}
\end{cases}
\qquad (91)
$$

Eventually, the dual sub-problem (63)-(88) can be recast as a MILP problem that can be solved using commercial solvers, e.g., CPLEX. Noted that, the decision variables of the dual sub-problem are $\Phi^{DS} = \left\{ z_{t,i}^{w\uparrow}, z_{t,i}^{w\downarrow}, \nu_t^{r+}, \nu_t^{r-}, P_{t,i}^{w,f} \right\} \cup \{(87),(88)\} \cup \{X_{t,i}^{r1+}, X_{t,i}^{r1-}, X_{t,i}^{r2+}, X_{t,i}^{r2-}, X_{t,i}^{w\uparrow}, X_{t,i}^{w\downarrow}\}$.

4.3. Pseudo-code flow diagram

For the sake of clarity, Algorithm 1 shows how the optimal solution of the proposed tri-level stochastic adaptive robust optimization approach is obtained under the nested C&CG algorithm.

Algorithm 1 : C&CG Algorithm for stochastic adaptive robust optimization approach.

Step 1) Initialization:
Lower bound (LB)= $-\infty$, Upper bound (UB)= $+\infty$, $\varepsilon = 10^{-6}$, $\chi \leftarrow 0$, and flag=no
Step 2) Solve the master problem (52), i.e., z^{MP*}, and obtain the optimal energy traded by the IEHS in the energy and reserve markets, i.e., $P_t^{da*}, P_t^{r+*}, P_t^{r-*}$.
     if $\chi = 0$
Skipped constraints (53)–(58) at first iteration.
Step 3) Update the upper bound, $UB = z^{MP*}$.
Step 4) Using the obtained optimal values in **Step 2**, solve the linear equivalent of the sub-problem (63), i.e., z^{SP*}, and determine the optimal dispatch of all equipment.
Step 5) Update the lower bound, $LB = max\{LB, z^{MP*} - \delta + z^{SP*}\}$.
     if $\frac{|UB-LB|}{UB} \leq \varepsilon$ **then**,
     flag=yes
     Else
Step 6) Update the iteration counter $\chi \leftarrow \chi + 1$.
Step 7) Fix ν_t^{r+*}, ν_t^{r-*}, and $P_{t,i}^{w,f*}$.
Step 8) Go to **Step 2** and repeat the nested structure.
     until stopping criterion is satisfied.

---

5. Case Studies

5.1. Test system and experiment settings

To assess the merit of the proposed tri-level stochastic adaptive robust optimization approach, a local IEHS is modeled by combining the IEEE-14 bus electric power system and HFSs, the layout of which is provided in Fig. 3. As illustrated, the IEHS hosts four HFSs, three WFs, one EVPL, and two FVPLs with different levels of pressure. Each HFS is made up of an electrolyzer, FC, and hydrogen storage. The peak electrical demand of individual consumers is considered to be 81 MW. The installed capacity of WF1, WF2, and WF3 are set to 30, 20, and 30 MW, respectively. The voltage magnitude threshold is set at ±5%, i.e., 0.95 *p.u.* and 1.05 *p.u.* The power factor for electrical demands is considered to be 0.65. Technical information about the power sector is taken from Abdolrasol et al. [2018]. The hourly power
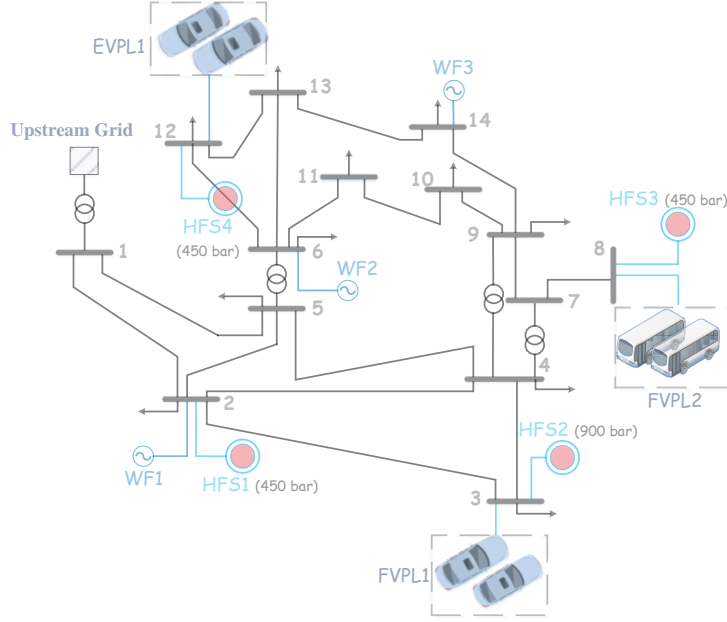
Fig. 3: The topology schematic of the IEHS employed in the case studies.

demand and expected level of available wind power generation are provided in Fig. 4. The day-ahead energy and up/down-reserve market prices are based on CAISO data on December 30, 2018, which are given in Fig. 5. Besides, the capacity prices in the regulation-up and down reserve markets, i.e., λ_t^{r+} and λ_t^{r-}, are considered equal to the average energy price in these markets. The maximum and minimum levels of bidding/offering quantity in the energy market are set between –75 and 75 MW, whereas these values are limited to –30 and 30 MW in each reserve market. The retail prices of electricity, i.e., π_t^{re}, is equal to $1.28 \times \lambda_t^{da}$ for selling power to individual consumers as well as equal to the lowest day-ahead energy market price for trading electricity with EVPLs Sadeghi et al. [2021]. The average price of hydrogen for a light-duty FCV currently is 17 \$/kg HCP [2023]. Thus, the retail price of hydrogen, i.e., π^{rh}, in the utility function of FCVs is assumed to be equal to this value. The hydrogen tank capacity is set to 500 kg and the mass of available hydrogen in the reservoir at the beginning of the scheduling period is assumed to be 50 kg. The operation range of the hydrogen storage is from 4% to 96%. The maximum charging/discharging level of the hydrogen storage is considered to be 50 kg. The variable operating cost coefficient of hydrogen storage is set as 10 \$/kg Khani et al. [2020]. Furthermore, the maximum rated capacity of electrolyzer and FC, i.e., $\overline{H^{gen}}$ and $\overline{H^{fc}}$, are taken as 320 and 10 kg, respectively. The travel behavior parameters (i.e., arrival and departure times) of each EV and FCV, charging rates, and battery capacities are presented in Table 2. In this study, the FCVs fleet consists of 60 buses and 100 private cars as well as the EVs fleet of 3500 taxis and 1200 business cars, whose behavior is modeled using the information presented in Table 2 and equations (14)-(18). The total number of vehicles parked in charging stations at each time slot as well as the arriving and departing SoE related to each station are sketched in Fig. 6.

According to the expected values of market prices, one thousand scenarios of electricity market prices are simulated by the Monte Carlo method. To reduce the computational burden of the optimization
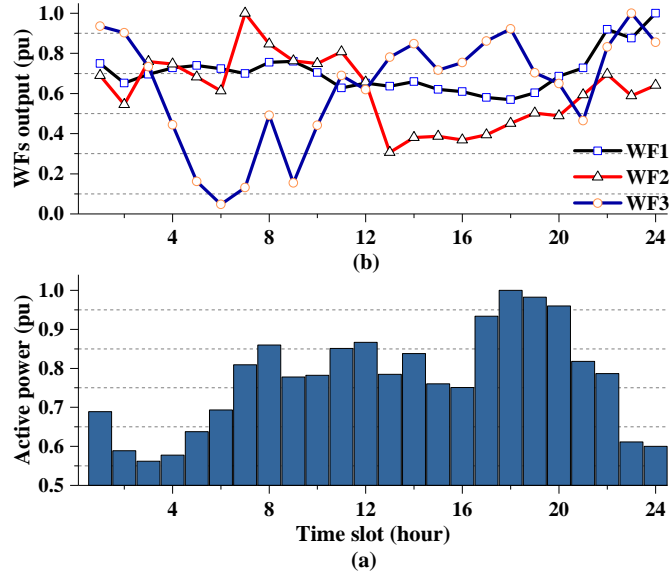
Fig. 4: Hourly data for (a) electrical demand and (b) output power of each WF.
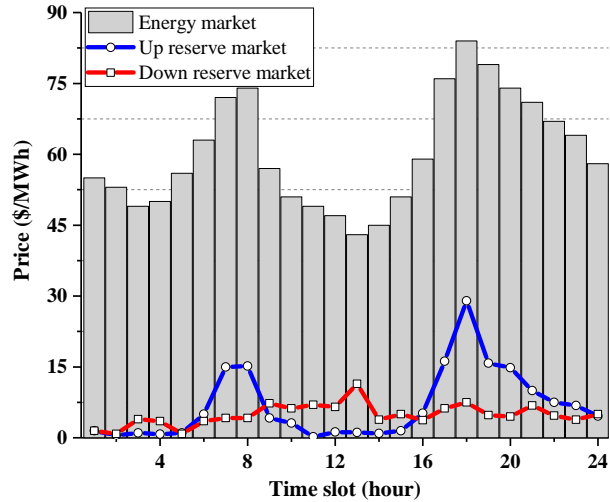
Fig. 5: Price information in day-ahead energy and regulation-up and down reserve markets.

problem, the generated scenarios are reduced to an appropriately small set of scenarios, i.e., ten scenarios, using the GAMS/SCENRED toolbox based on the probability of occurrence of different situations. The decision to limit the scenario set to ten has been made based on a careful balance between computational efficiency and the need for adequate scenario representation. This ensures that the optimization problem remains solvable within reasonable computational resources while still capturing a diverse range of uncertainty instances. While a larger number of scenarios may provide finer granularity in capturing uncertainty, it also significantly increases computational burden without necessarily proportionally improving solution accuracy. Moreover, to apply the stochastic adaptive robust optimization approach, the maximum deviation between the expected and actual value of wind power generation is fixed at 20%. It should be noted that the out-of-sample testing is performed to validate the robustness of our stochastic adaptive robust optimization approach. Out-of-sample testing involves assessing the performance of the
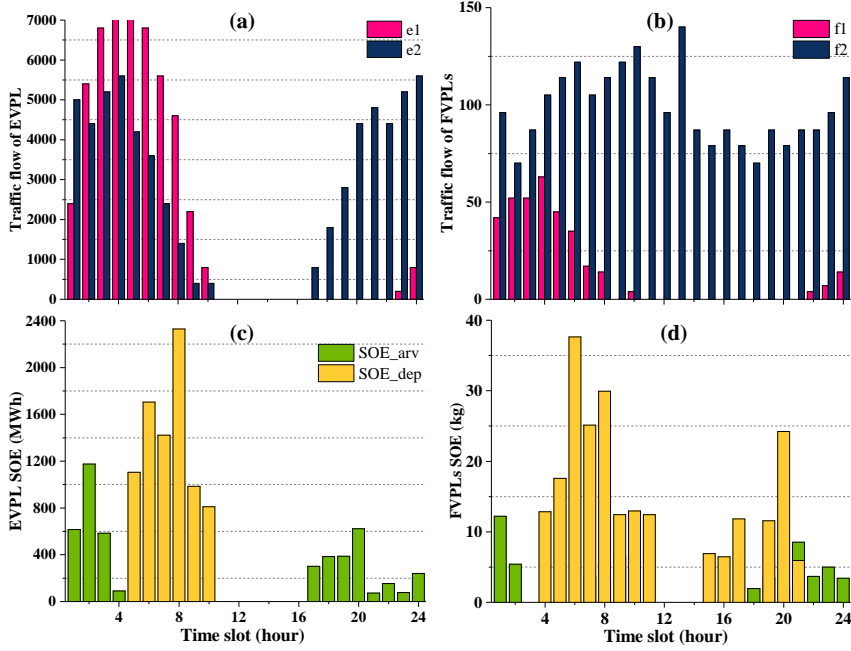
Fig. 6: Distribution of parked vehicles in each (a) EVPL and (b) FVPL. The total arriving and departing SoE of (c) EVPL and (d) FVPL.

optimization model using scenarios that were not included in the training set. This helps evaluate the generalization ability of the model and its ability to handle unseen instances of uncertainty effectively.

Three cases, which emphasize the importance of the nexus operation of the electricity-hydrogen systems in the electricity markets and assess the financial risks involved in market transactions, are studied as follows:

- *Case 0:* Applying the market-oriented model only to determine the bidding/offering strategy of the *power sector* in day-ahead energy and reserve electricity markets taking into account the pure stochastic programming approach. In this case, the role of HFSs and the mobility sector does not consider in the market participation strategy as well as the uncertainty of wind power generation and calls for reserve service are skipped.

- *Case 1:* Developing *Case 0* to determine the profit-seeking behavior of *IEHS* in day-ahead energy and regulation-up and down reserve markets considering the mobility sector.

- *Case 2:* *Case 1* is developed by considering the proposed tri-level stochastic adaptive robust optimization approach to determine the optimal bidding/offering strategy for IEHS in both energy and reserve markets. This case is established to show how the profit of the IEHS will change when the uncertainties of wind power generation and calls for reserve service are put into the market-oriented model. To accurately analyze this case and compare the results, the budget of uncertainty for wind power generation and reserve deployment requests, i.e., Γ^w and Γ^r, are fixed to 8 and 8, respectively.

The defined optimization cases, compiled as a MILP model, are run on a laptop with an Intel Core i7-4500 CPU 1.8 GHz with 6 GB of RAM in GAMS software with commercially available solver CPLEX 12.10. Both relative and absolute optimization gaps are zero when the GAMS option Optcr is set to zero. The

Table 3: Expected profit evaluation report for each case (note $K=$1000).

Case no.	Case 0	Case 1	Case 2
Revenue (or cost) allocated to energy market transactions ($k)	-16.219	21.257	1.797
Revenue allocated to reserve markets transactions ($k)	0.068	6.849	3.847
Revenue from power sales to individual consumers ($k)	117.805	117.805	117.805
Revenue from trading power/hydrogen with mobility sector ($k)	-	130.358	130.358
Operation cost of hydrogen storage ($k)	-	1.191	1.131
Expected profit ($k)	101.654	275.078	252.676

simulation results arising from these cases are summarized in the following sub-sections, in which the scheduling horizon is considered 24 hours with 1-hour granularity.

5.2. Simulation results and discussion

5.2.1. IEHS's scheduling results

To compare the economic viability of the IEHS with the traditional power system in the day-ahead energy and reserve electricity markets, different financial terms are reported in Table 3. It is shown that the expected economic profit of *Case 1* is higher than *Case 0* by 170.6%. This indicates the benefits of considering HFSs and the mobility sector as economic stimulus in bidding/offering strategies of the power sector in a coordinated manner. As evident from Table 3, in *Case 0*, the system operator not only does not benefit from the economic opportunities of the energy market, but also has to pay $16.219k to meet the individual consumers' demands. As expected, the operator offers the lowest operating reserve capacity to the regulation-up and down reserve markets in *Case 0*, resulting in a revenue of $0.068k. In contrast, the IEHS operator earns the highest revenue ($6.849k) from power trades in the reserve markets in *Case 1*. These results clearly demonstrate that ignoring the HFSs and the mobility sector in coordination with the power sector could cause severe economic losses for an IEHS operator. It is insightful to compare the outcomes of the bidding/offering strategy for IEHS with (i.e., *Case 2*) and without (i.e., *Case 1*) adopting the developed stochastic adaptive robust optimization approach. The expected economic profit decreases to $252.676k in *Case 2* when the developed stochastic adaptive robust optimization approach is adopted, which is 8.14% lower than the obtained value under *Case 1*. However, even with a relatively high degree of robustness in *Case 2*, this case is still superior than *Case 0*, because the coordinated use of HFSs, especially FCs, hydrogen storage, and FCVs, and power sector increases the reserve capacity to manage risks arising from uncertain parameters. Since the first term belongs to reserve markets in (49) (i.e., $\lambda_t^{r+} P_t^{r+} + \lambda_t^{r-} P_t^{r-}$) is not affected by the uncertainty parameters, the IEHS operator has maintained its tendency to offer operating reserve capacity in these markets in *Case 2* (40% reduction in reserve supply compared to *Case 1*).

The bidding/offering strategy of IEHS in energy and reserve markets in cases 1 and 2 are respectively presented in Figs. 7 and 8. In Fig. 7, the positive value indicates the purchased power from energy market and the negative amount demonstrates the sold power to this market. These figures show that due to the profitability of energy and up-reserve markets, the IEHS operator is more willing to participate in these markets and adjusts the operation of WFs, EVPL, FCs, and electrolyzers with the aim of trading as much power as possible in these markets. To do this, the IEHS tries to keep the output power of FCs close to their minimum generation level to offer the unused capacity in the up-reserve market. Similarly, IEHS keeps the parked vehicles in EVPLs in charging mode so that it can offer the available capacity

in the EVPL in the up-reserve market (see Fig. 9(a)). It can also be inferred from Figs. 7 and 4 that the participation rate of IEHS in the energy market follows the expected level of available wind power generation and demands of individual consumers. As seen from these figures, at the beginning and end of the scheduling horizon, the load demand falls into the valley periods and the available wind power generation is higher than other periods, therefore more power is to be offered to the energy market to maximize the worst-case expected profit. In contrast, during time intervals 6-21, the load demand falls into the peak periods and the available wind power generation drops, resulting in less power to be offered to the energy market. In *Case 2*, according to the defined level of risk in the stochastic adaptive robust optimization approach, the IEHS operator must make more conservative decisions about the available wind power generation, so the amount of power sold to the energy market is decreased by up to 24% compared to *Case 1*. As can be seen from Fig. 7 for *Case 2*, during time intervals 6-9 and 18-22, instead of offering the power to the energy market, IEHS purchases the power from this market so that if the wind power output deviates from the forecasted value, the power demands will be continuously supplied without any interruption. The consistent purchasing behavior in the energy market suggests that the IEHS relies heavily on external sources for energy supply. The resulting strategy for the IEHS can be justified depending on factors such as cost-effectiveness, risk aversion, and flexibility in meeting the energy demands. The centralized self-scheduling strategy is affected by the operational limitations of various components within the IEHS, including HFSs, EVPLs, and WFs, and the optimization of hydrogen-based resource allocation within the HFSs in balancing energy and reserve market participation. As can be seen from Fig. 8, scheduled participation in the up-reserve market is at the maximum level, i.e., 30 MW, at most time slots. This behavior indicates that the IEHS is contributing to the provision of upward reserve capacity to the grid. Due to the level of risk-taking for calls for reserve service, the participation rate in the up-reserve market in *Case 2* is different from *Case 1* at seven time slots. In contrast, the minimum participation rate is assigned to the down-reserve market where the scheduled participation is zero for most time periods. It can be inferred that the behavior of the IEHS is fully dependent on the risk management strategies associated with reserve market participation, including considerations of capacity availability, price dynamics, and operational constraints.

For more detailed analysis, Fig. 9 illustrates the power and hydrogen exchange rate between IEHS and the EVPL/FVPLs in *Case 1*. As observed, in most of the time slots, the IEHS operator tries to bring the state of charge level of parked vehicles to the desired level, i.e., $SOC_{(\cdot)}^{des}$, by injecting power/hydrogen into the parking lots. This fact is clearly seen in the fourth line of Table 3, where the IEHS operator earns significant revenue from the energy trading with the mobility sector ($130.358k). On the other hand, during the peak price periods, i.e., 7-10 and 17-24, EVPLs operate in discharge mode and directly help the IEHS to meet consumers' demands without purchasing power from the energy market (see Fig. 7).

5.2.2. Impact of power sector congestion

In the practice, the power sector is subjected to different contingencies, and it is interesting to show how sensitive the performance of the developed tri-level stochastic adaptive robust optimization approach is to the selection of power grid parameters. To this end, the sensitivity of the expected profit as well as
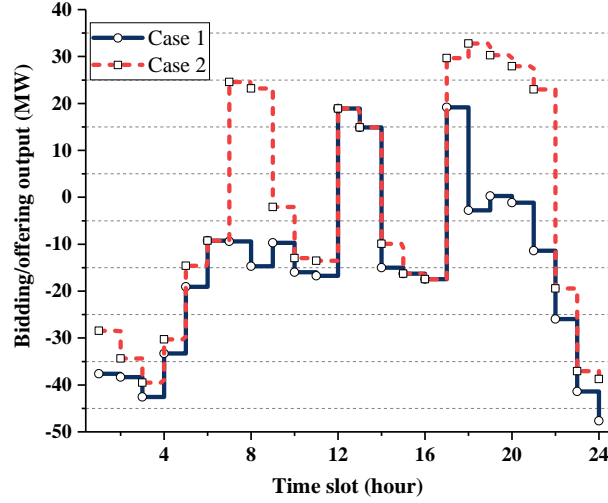
Fig. 7: Bidding/offering strategy of IEHS in energy market for cases 1 and 2.
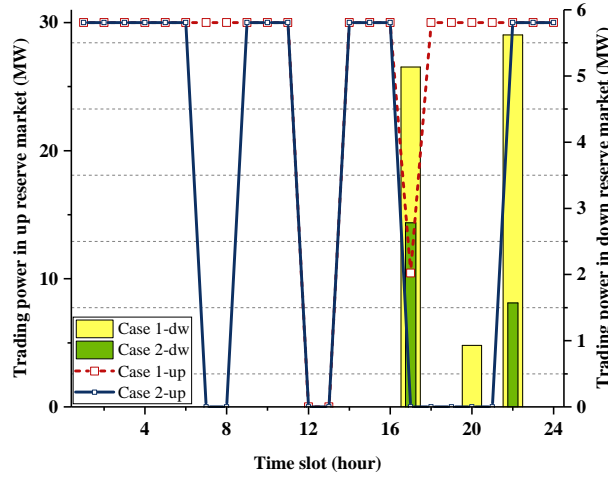
Fig. 8: Bidding/offering strategy of IEHS in reserve markets for cases 1 and 2.

the mass of hydrogen delivered to HFSs to the power line capacity is examined for *Case 2*. The results are illustrated in Fig. 10, where the capacity of power lines has been changed from 100% to 60% of nominal capacity. As observed, when the power sector is heavily congested, e.g., 70%-60% of nominal line capacity, there will be less space for power trading with day-ahead electricity markets, which will influence the amount of electric power converted to hydrogen. From an economic point of view, the expected profit of IEHS remains almost unchanged up to values close to 70% of nominal line capacity. But, this value drops from $252.6k to $249.4k with reducing the capacity of power lines to more than 60% of nominal capacity. Whereas it is seldom possible for the power sector to suffer from such severe congestion, the economic results demonstrate that the proposed bidding/offering strategy is much more computationally efficient during normal and contingency conditions.

5.2.3. Influence of mobility sector on IEHS's bidding/offering strategy

Herein, the influences of different scales of the mobility sector on the expected profit of IEHS as well as the amount of traded power between IEHS and energy market are evaluated, the results of which are

27
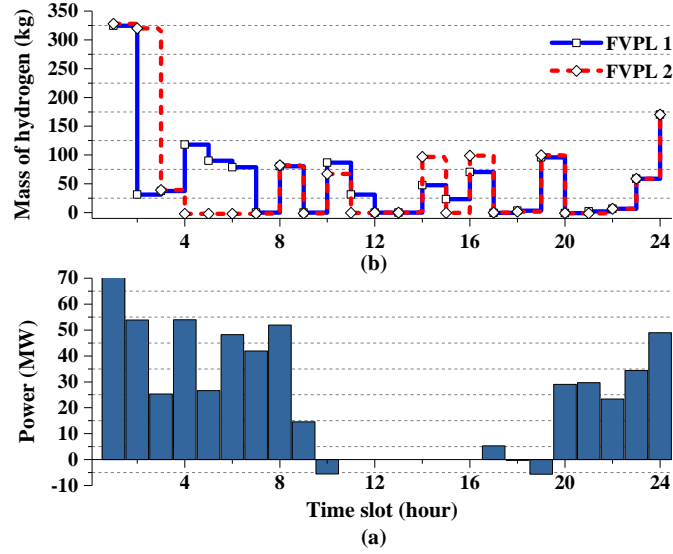
Fig. 9: Amount of power/hydrogen exchange between IEHS and (a) EVPL, (b) FVPLs for case 1.
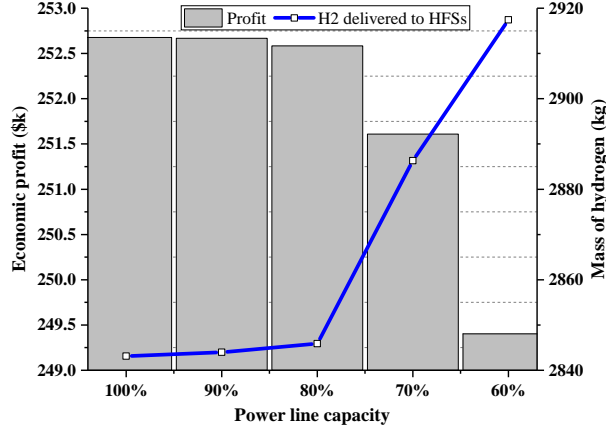
Fig. 10: Influence of power line capacity on IEHS profit and mass of hydrogen delivered to HFSs.

shown in Fig. 11. All settings are the same as those of *Case 2*. Some interesting observations can be made from this analysis. The most important thing that can be deduced is that the IEHS tends to focus on energy exchange with the mobility sector and decreases the participation rate in the energy market. This is due to the existence of severe uncertainty sources on the market side, i.e., electricity market prices and calls for reserve service, which can pose significant economic threats for the IEHS. Also, due to physical limitations, the profit of the IEHS has limited scalability of the number of vehicles parked in parking lots. For instance, the profit of the IEHS remains constant with increasing the scale of the mobility sector to more than 50% of the initial values. The reason is that the IEHS operator initially attempts to entirely exploit the generation of WFs directly to meet the demands of EVPL and/or indirectly (i.e., green hydrogen production) to cover the demands of FVPLs. And since the operator is reluctant to purchase power from the energy market, therefore it tries to keep the state of charge level of all vehicles when leaving the parking lots only at the desired level and no more.

The growth of EVs and FCVs fleet will necessitate a very high diffusion of IEHSs. Since each IEHS must have a separate operator, hence the proposed robust bidding/offering strategy can be implemented

28
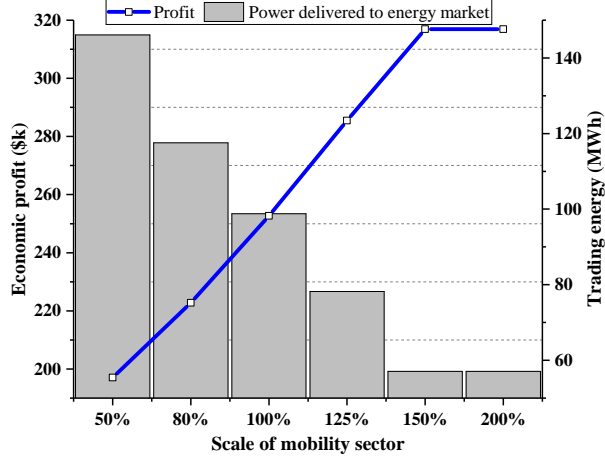
Fig. 11: Influence of scales of mobility sector on IEHS profit and power trading with energy market.

separately for each system. This indicates the high importance of this study.

5.2.4. Impact of risk level on IEHS performance

In this sub-section, the impacts of the budget of uncertainty parameters, i.e., Γ^w and Γ^r, which are used to handle the uncertainties of wind power generation and calls for reserve service, on the results of the bidding/offering strategy are investigated. The variations in the expected profit of the IEHS when Γ^w and Γ^r change from 0 to 20 are shown in Fig. 12. It can be inferred from this figure that there are profit reductions for IEHS operator with the increase in the budget of uncertainty parameters as the risk factor. Clearly, such declines can be manifested as an expected phenomenon as a result of reducing the amount of financial risk. Accordingly, the IEHS operator tries to choose the worst-case dispatch decisions to mitigate the economic risks emanating from more severe prediction violations.

Moreover, the variation in the amount of traded power between the energy market and IEHS for different robustness degrees is illustrated in Fig. 13. To perform this analysis, four different (Γ^w, Γ^r) combinations, i.e., (4, 16), (8, 8), (16, 8), and (20, 20), are selected to repeat *Case 2*. Suppose (20, 20) and (4, 16) combinations to give a better insight into the impact of these two parameters on the traded power in the energy market. As one would expect, as the robustness degree increases, the IEHS operator is less inclined to offer power to the energy market, and the operator strives to make the most conservative decisions to participate in the day-ahead electricity markets to meet its obligations with the least loss. As can be seen in Fig. 13, the power offered to the energy market in (4, 16) combination is 270 MWh, which is reduced by half for (20, 20) combination. This trend might become more pronounced depending on the robustness degree intended for the uncertainty sources. It can be deduced that with respect to the developed risk-constrained bidding/offering strategy, the opportunity for adoption of different patterns is available for IEHS to deal with scenarios that model vacillations of wind power generation, market prices, and reserve service requests.

5.2.5. After-the-fact analysis

As previously delineated, the tri-level stochastic adaptive robust optimization framework developed in this study is herein termed as a "worst-case performance" methodology. Its objective is to minimize
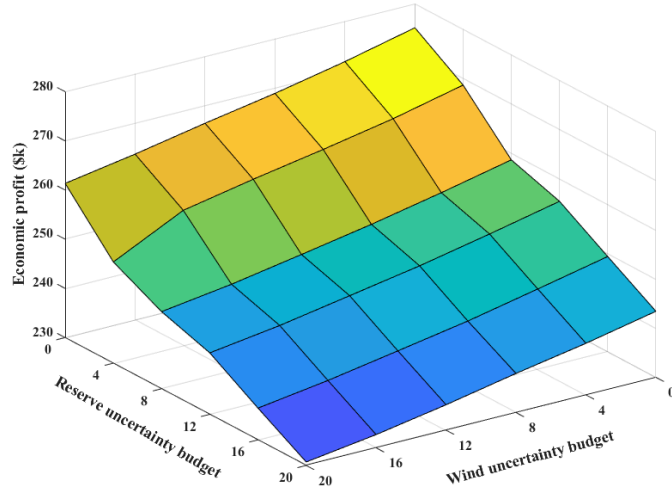
Fig. 12: Impact of Γ^w and Γ^r on the expected profit of IEHS for case 2.
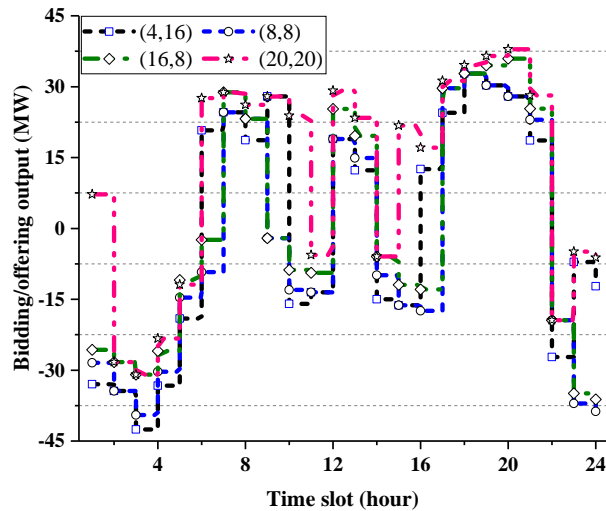
Fig. 13: Sensitivity of the traded power in the energy market to the budget of uncertainty for wind power generation and reserve deployment requests (Γ^w, Γ^r).

the anticipated profit of IEHSs while considering the uncertainty budget parameter and the maximum deviation from predicted values Oskouei et al. [2021]. Conversely, stochastic methodologies endeavor to address the uncertain nature of various parameters by relying on a finite set of scenarios. In this sub-section, the efficacy and applicability of the proposed tri-level stochastic adaptive robust optimization approach to optimally determine the bid/offer strategy for IEHSs is evaluated through a retrospective analysis juxtaposed with a purely stochastic approach. As outlined in Fig. 12, the economic profit in the worst-case scenario, i.e., employing the developed tri-level stochastic adaptive robust approach in *Case 2* with the uncertainty budget for wind power generation and reserve deployment requests, i.e., Γ^w and Γ^r, set at 20, is equal to $230.17k. This represents the most pessimistic situation possible in real-time sessions, and the IEHS's profit cannot be less than this value in the face of all uncertain sources. After that, the uncertainties of wind power generation and calls for reserve service are modeled with several scenarios, such as the electricity market price, to solve the risk-constrained bidding/offering problem for IEHSs using the pure stochastic approach. The assumptions are similar to *Case 2*, but the adaptive
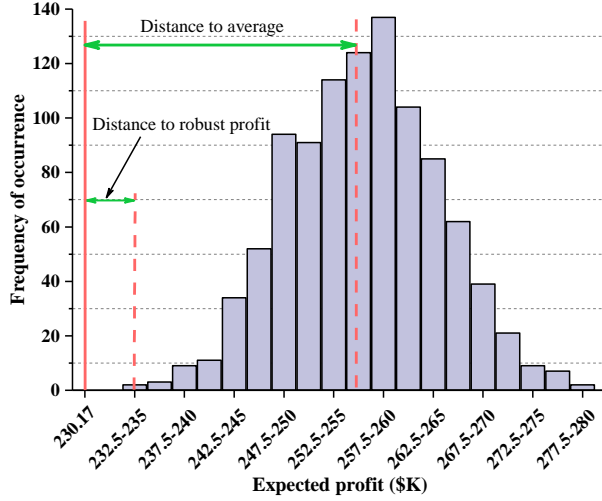
Fig. 14: After the fact analysis to justify the robustness of the developed tri-level stochastic adaptive robust approach.

robust approach is not used. Instead, a scenario-based stochastic optimization method is employed to control all uncertainty parameters. To this end, one thousand scenarios are synthetically generated using the Monte Carlo Simulation technique to model wind power generation and up and down-reserve capacity coefficient requested by ISO, in conjunction with market price dynamics. It is imperative to highlight that the predicted wind power generation in Fig. 4(b) serves as the base value for scenario creation. Subsequently, the expected profit of the IEHS is derived by solving the conventional two-stage stochastic optimization problem individually for each scenario set. In this context, equations (1)-(42) are adapted into a formulation representing a two-stage stochastic optimization problem, thus forming the core of the optimization process aimed at determining the optimal bidding/offering strategy for the participation of the IEHS in energy and reserve markets. The outcomes of the after-the-fact analysis are presented in Fig. 14. As seen from Fig. 14, the expected profit of the IEHS is consistently higher than the value obtained by the tri-level stochastic adaptive robust optimization approach, which was \$230.17k. The conducted after-the-fact analysis revealed three key profit metrics: the minimum profit of the IEHS (\$232.5k), the average profit of the IEHS (\$256.25k), and the maximum profit of the IEHS (\$280k). These metrics represent the range of possible outcomes under different realizations of uncertainty. It can be concluded that the tri-level stochastic adaptive robust optimization approach focuses on maintaining performance under worst-case uncertainty realizations. This means that the decisions made are resilient to extreme scenarios, ensuring a certain level of performance even in adverse conditions. In contrast, the scenario-based stochastic approaches may not explicitly address worst-case scenarios unless specifically designed to do so. Furthermore, the tri-level stochastic adaptive robust optimization approach aims to find solutions that perform well across a range of possible scenarios without overfitting to specific historical data or simulated scenarios, providing more generalizable and robust solutions. Overall, it can be confirmed that the tri-level stochastic adaptive robust optimization approach offers a more proactive and resilient strategy for managing uncertainties in IEHS systems, ensuring stable profits even under worst-case scenarios in real-time operations.

5.2.6. Net present value (NPV) analysis

This study primarily focuses on the optimal participation of IEHSs in day-ahead energy and reserve markets, with an emphasis on maximizing expected profit. However, since this study revolves around optimizing an IEHS that has not yet been established, it is crucial to consider the investment cost of the system. Even if the operational strategy is optimized, investors may struggle to recover the construction costs. The establishment of IEHSs involves substantial capital investments. Assuming that the infrastructure of the power sector does not need to be strengthened, the essential investments to establish such systems include the placement of hydrogen production units, i.e., electrolyzers, storage systems, and FCs to convert hydrogen into power at HFSs. It is insightful to evaluate the economic justification of establishing IEHSs in providing a more comprehensive understanding of the economic viability and practicality of the proposed IEHSs in the long term as well as attracting investment flows. To this end, the net present value (NPV) analysis is contemplated to evaluate the economic viability of IEHSs over their lifespan. The NPV analysis enables policy-makers and decision-makers to make far-sighted decisions regarding the installation of hydrogen-based facilities for the development of green energy systems. Through this analysis, the payback period can be determined by calculating the difference between the initial investment and the present value of cash flows. The NPV method could be declared mathematically by (92). In (92), IC_0 represents the initial investment costs of all FCs, PEM electrolyzers, and hydrogen storage systems deployed in the studied IEHSs. As shown in Fig. 3, the considered IEHS is made up of four electrolyzers, four FCs, and four hydrogen storage systems. Therefore, the financial value of all these pieces of equipment should be considered to calculate the initial investment costs. Moreover, term $IEHS_{profit}$ represents the daily profit of the IEHS operator, as stated in (49). ε denotes the discount rate, which is set to 10% in the conducted analysis. n expresses the payback period.

$$NPV = -IC_0 + \left[\frac{(1+\varepsilon)^n - 1}{\varepsilon(1+\varepsilon)^n} \times 365 \times \text{IEHS}_{\text{profit}} \right] \tag{92}$$

The NPV of the proposed risk-constrained bidding/offering strategy for IEHSs for *Case 2* is depicted in Fig. 15. In the carried-out analysis, the corresponding capital costs for FC, hydrogen storage, and electrolyzer are considered to be 3000 \$/kW, 2.3 \$/kg, and 1400 \$/kW, respectively CESA [2023]; NREL [2023]. As can be seen from Fig. 15, the cumulative NPV becomes positive from the seventh year, which positive NPV indicates that the project is economically viable and its benefits outweigh the investment costs. Therefore, the payback period for establishing the studied IEHS is seven years. This analysis confirms the economic competence of developing IEHSs and demonstrates that these systems can become an attractive investment choice for stakeholders committed to a clean energy future. Furthermore, the economic justification for establishing IEHSs in the long term is fully supported given their ability to improve energy efficiency, align with energy market trends and policies, reduce environmental impacts, and create diversified revenue streams. It should be noted that the accurate performance of NPV analysis requires the consideration of all financial flows. Nevertheless, to avoid any ambiguity and unreasonable assumptions, the NPV analysis is limited to the initial investment costs and the daily profits obtained by the IEHS through participation in the day-ahead energy and reserve markets.
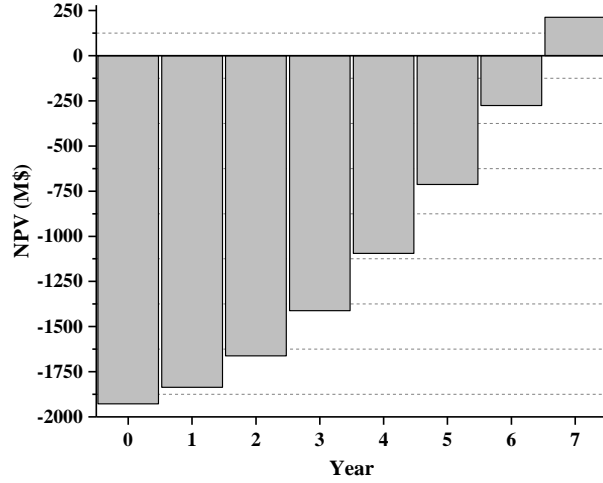
Fig. 15: NPV of the developed market-oriented strategy for case 2.

5.3. Implementation and limitations

The proposed strategy has some limitations. First, determining the optimal capacity of the IEHSs components with respect to investment and recovery costs is a prerequisite for the implementation of the proposed strategy in commercial operations. This issue requires the development of a model to simultaneously address the planning and scheduling problems of IEHSs. However, we acknowledge that this study is only limited to presenting a robust scheduling approach and does not address the investment costs incurred by the IEHS's operator. Second, the IEHSs have been considered as price-taker units for implementing the self-scheduling problem. Sometimes, these entities may participate as price-maker units in the electricity market. In this case, the developed methodology should be expanded and the day-ahead electricity market price should be defined as a variable in the framework of a bi-level problem. Third, the presented strategy does not represent the inaccuracy of the approximations in the reserve capacity coefficient requested by ISO and the synergistic effects of the transportation and power networks on the robust operation of IEHSs. All these limitations can have a significant impact on the outcomes of the simulations. Deriving such proof and their technical and economic justification can be the future research direction.

However, it is crucial to address scalability concerns to ensure the practical applicability of the proposed strategy in larger-scale IEHS environments. The proposed risk-constrained bidding/offering problem for IEHSs leverages advanced optimization techniques and algorithmic optimizations to ensure computational tractability even for complex, real-world IEHSs. Furthermore, utilizing the adaptive robust method in conjunction with techniques such as scenario reduction can reduce computational burden while maintaining solution quality. To further enhance scalability, the proposed approach can be parallelized and implemented using distributed computing frameworks. This enables the solution process to be distributed across multiple computing nodes, effectively reducing solution times for large-scale systems. Moreover, identifying and prioritizing the most critical aspects of IEHS operation can streamline the optimization process without sacrificing essential system dynamics.

6. Conclusions and Future Work

This paper unveiled a risk-constrained bidding/offering problem for IEHSs in coordination with the mobility sector to simultaneously participate in day-ahead energy and regulation-up and down reserve markets. The IEHSs hosted the power sector, intermittent renewable generations, as well as HFSs containing FCs, electrolyzers, and hydrogen storage units. In line with the market-oriented plan designed for IEHSs, a win-win strategy was developed to encourage the mobility sector's actors, i.e., owners of EVs and FCVs, to cooperate with IEHSs, taking into account the utility functions of owners and important human-related factors. In addition, the uncertainties of wind power generation, electricity market prices, and calls for reserve service were handled through a tri-level stochastic adaptive robust optimization approach to manage economic risks arising from these uncertain sources. By adopting these measures, not only will the proposed strategy be able to achieve highly accurate optimal solutions, but also the proposed strategy will become much more reliable and realistic. The computational results showed that the simultaneous optimization of the mobility sector along with other power and hydrogen prosumers can lead to a sharp increase in the expected profit of IEHS operator from \$101.654k to \$275.078k. The use of HFSs, in addition to increasing the income from power exchange in the reserve market from \$0.068k to \$6.849k, also played an undeniable role in maintaining the stable performance of IEHSs in case of congestion occurrences in the power sector. Other salient results of this study include the very low dependence of the IEHS's profit on the adoption of a high degree of robustness to address uncertain parameters and technical parameters of the power sector, such as line capacity.

According to the key findings of this study, it can be stated that hydrogen-based facilities have a potential role in balancing the power sector and developing international trade. The implementation of IEHSs at the practical level requires the scaling up of hydrogen storage systems and hydrogen production units as new distributed applications. In this regard, several research projects are being completed to develop hydrogen storage systems at different scales rapidly, e.g., HyCAVmobil in Germany and HyPSTER in France, both of which will start practical tests by the beginning of 2024. With the development of the necessary infrastructure by the leading countries in the field of green hydrogen, the technical value of the present study will be objectively tangible in enhancing the flexibility level of energy systems in practical applications. In addition, as a step towards the practical development of IEHSs, operators can monitor the charging behavior of self-owned parking lots over a period, and then use machine learning techniques to forecast the mentioned human-related factors for purposeful participation in day-ahead electricity markets. Addressing this issue will be considered as part of future work.

References

Abdolrasol, M. G. M., Hannan, M. A., Mohamed, A., Amiruldin, U. A. U., Abidin, I. B. Z., & Uddin, M. N. (2018). An optimal scheduling controller for virtual power plant and microgrid integration using the binary backtracking search algorithm. *IEEE Transactions on Industry Applications*, *54*, 2834–2844.

Akbari, T., & Tavakoli Bina, M. (2016). Approximated MILP model for AC transmission expansion

planning: global solutions versus local solutions. *IET Generation, Transmission & Distribution*, *10*, 1563–1569.

Akhavan-Hejazi, H., & Mohsenian-Rad, H. (2018). Energy storage planning in active distribution grids: A chance-constrained optimization with non-parametric probability functions. *IEEE Transactions on Smart Grid*, *9*, 1972–1985.

Ban, M., Yu, J., Shahidehpour, M., & Yao, Y. (2017). Integration of power-to-hydrogen in day-ahead security-constrained unit commitment with high wind penetration. *Journal of Modern Power Systems and Clean Energy*, *5*, 337–349.

Baringo, A., & Baringo, L. (2017). A stochastic adaptive robust optimization approach for the offering strategy of a virtual power plant. *IEEE Transactions on Power Systems*, *32*, 3492–3504.

Coffrin, C., & Van Hentenryck, P. (2014). A linear-programming approximation of AC power flows. *INFORMS Journal on Computing*, *26*, 718–734.

El-Taweel, N. A., Khani, H., & Farag, H. E. Z. (2019). Hydrogen storage optimal scheduling for fuel supply and capacity-based demand response program under dynamic hydrogen pricing. *IEEE Transactions on Smart Grid*, *10*, 4531–4542.

Firtina-Ertis, I., Acar, C., & Erturk, E. (2020). Optimal sizing design of an isolated stand-alone hybrid wind-hydrogen system for a zero-energy house. *Applied Energy*, *274*, 115244.

Floudas, C. A. (1995). Nonlinear and mixed-integer optimization: fundamentals and applications. *New York, NY, USA: Oxford Univ. Press*, .

Haggi, H., Sun, W., Fenton, J. M., & Brooker, P. (2021). Risk-averse cooperative operation of PV and hydrogen systems in active distribution networks. *IEEE Systems Journal*, (pp. 1–10).

Kachirayil, F., Weinand, J. M., Scheller, F., & McKenna, R. (2022). Reviewing local and integrated energy system models: insights into flexibility and robustness challenges. *Applied Energy*, *324*, 119666.

Khani, H., El-Taweel, N. A., & Farag, H. E. Z. (2020). Supervisory scheduling of storage-based hydrogen fueling stations for transportation sector and distributed operating reserve in electricity markets. *IEEE Transactions on Industrial Informatics*, *16*, 1529–1538.

Li, B., Chen, M., Ma, Z., He, G., Dai, W., Liu, D., Zhang, C., & Zhong, H. (2022). Modeling integrated power and transportation systems: Impacts of power-to-gas on the deep decarbonization. *IEEE Transactions on Industry Applications*, *58*, 2677–2693.

Li, J., Lin, J., Zhang, H., Song, Y., Chen, G., Ding, L., & Liang, D. (2020). Optimal investment of electrolyzers and seasonal storages in hydrogen supply chains incorporated with renewable electric networks. *IEEE Transactions on Sustainable Energy*, *11*, 1773–1784.

Li, Z., Wu, L., Xu, Y., Wang, L., & Yang, N. (2023). Distributed tri-layer risk-averse stochastic game approach for energy trading among multi-energy microgrids. *Applied Energy*, *331*, 120282.

Mu, Y., Wang, C., Cao, Y., Jia, H., Zhang, Q., & Yu, X. (2022). A cvar-based risk assessment method for park-level integrated energy system considering the uncertainties and correlation of energy prices. *Energy*, *247*, 123549.

Oskouei, M. Z., Mohammadi-Ivatloo, B., Abapour, M., Shafiee, M., & Anvari-Moghaddam, A. (2021). Strategic operation of a virtual energy hub with the provision of advanced ancillary services in industrial parks. *IEEE Transactions on Sustainable Energy*, *12*, 2062–2073.

Sadeghi, S., Jahangir, H., Vatandoust, B., Golkar, M. A., Ahmadian, A., & Elkamel, A. (2021). Optimal bidding strategy of a virtual power plant in day-ahead energy and frequency regulation markets: A deep learning-based approach. *International Journal of Electrical Power & Energy Systems*, *127*, 106646.

Sauer, W. (2014). Uplift in RTO and ISO markets. *Federal Energy Regulatory Commission, Washington, DC, USA, Technical Report*, .

Shao, C., Feng, C., Shahidehpour, M., Zhou, Q., Wang, X., & Wang, X. (2021). Optimal stochastic operation of integrated electric power and renewable energy with vehicle-based hydrogen energy system. *IEEE Transactions on Power Systems*, *36*, 4310–4321.

Sun, G., Li, G., Li, P., Xia, S., Zhu, Z., & Shahidehpour, M. (2022). Coordinated operation of hydrogen-integrated urban transportation and power distribution networks considering fuel cell electric vehicles. *IEEE Transactions on Industry Applications*, *58*, 2652–2665.

Tao, Y., Qiu, J., Lai, S., & Zhao, J. (2021). Integrated electricity and hydrogen energy sharing in coupled energy systems. *IEEE Transactions on Smart Grid*, *12*, 1149–1162.

CESA (2023). Clean energy states alliance, [online]. available at: https://www.cesa.org/wp-content/uploads/cesa-fuelcelltechnology-may2010.pdf/, .

FCW (2022). Fuel cells works, [online]. available at: https://www.fuelcellsworks.com/news/russia-ukraine-war-will-accelerate-move-to-green-hydrogen-renewable-energy-plug-power-ceo/, .

HCP (2023). Hydrogen central price news, [online]. available at: https://www.hydrogenfuelnews.com/why-is-hydrogen-fuel-so-expensive/8558411/, .

ICCT (2021). Charging up America, assessing the growing need for u.s. charging infrastructure through 2030, international council on clean transportation, .

IEA (2022). International energy agency, [online]. available at: https://www.goldmansachs.com/intelligence/pages/gs-research/green-hydrogen/report.pdf/, .

ITM POWER PLC (2022). [online]. available at: https://www.itm-power.com/projects/h2mobility/, .

NREL (2023). National renewable energy laboratory, [online]. available at: https://www.nrel.gov/docs/fy14osti/58564.pdf/, .

Xiao, D., Lin, Z., Chen, H., Hua, W., & Yan, J. (2024). Windfall profit-aware stochastic scheduling strategy for industrial virtual power plant with integrated risk-seeking/averse preferences. *Applied Energy*, *357*, 122460.

Xiao, Y., Wang, X., Pinson, P., & Wang, X. (2018). A local energy market for electricity and hydrogen. *IEEE Transactions on Power Systems*, *33*, 3898–3908.

Xuan, A., Shen, X., Guo, Q., & Sun, H. (2021). A conditional value-at-risk based planning model for integrated energy system with energy storage and renewables. *Applied Energy*, *294*, 116971.

Yang, D., He, S., Wang, M., & Pandžić, H. (2020). Bidding strategy for virtual power plant considering the large-scale integrations of electric vehicles. *IEEE Transactions on Industry Applications*, *56*, 5890–5900.

Yin, X., Zhao, Z., & Yang, W. (2023). Ensemble prediction aided multi-objective co-design optimizations of grid-connected integrated renewables for green hydrogen production. *Journal of Cleaner Production*, *425*, 138585.

Zare Oskouei, M., & Gharehpetian, G. B. (2024). Flexibility enhancement of multi-district discos considering a trade-off between congestion and extractable reserve capacity from virtual energy storage systems. *Applied Energy*, *353*, 122181.

Zare Oskouei, M., & Mehrjerdi, H. (2022). Optimal allocation of power-to-hydrogen units in regional power grids for green hydrogen trading: Opportunities and barriers. *Journal of Cleaner Production*, *358*, 131937.

Zare Oskouei, M., Mehrjerdi, H., Babazadeh, D., Teimourzadeh Baboli, P., Becker, C., & Palensky, P. (2022). Resilience-oriented operation of power systems: Hierarchical partitioning-based approach. *Applied Energy*, *312*, 118721.

Zare Oskouei, M., Mohammadi-Ivatloo, B., Abapour, M., Shafiee, M., & Anvari-Moghaddam, A. (2021). Techno-economic and environmental assessment of the coordinated operation of regional grid-connected energy hubs considering high penetration of wind power. *Journal of Cleaner Production*, *280*, 124275.

Zhang, K., Zhou, B., Chung, C. Y., Bu, S., Wang, Q., & Voropai, N. (2022). A coordinated multi-energy trading framework for strategic hydrogen provider in electricity and hydrogen markets. *IEEE Transactions on Smart Grid*, (pp. 1–1).